# Strong specific anti-viral responses in pediatric COVID-19 patients in South Brazil

**Tiago Fazolo**
Departamento de Ciências Básicas da Saúde, Universidade Federal de Ciências da Saúde de Porto Alegre - UFCSPA. https://orcid.org/0000-0001-6560-7004

**Karina Lima**
Departamento de Ciências Básicas da Saúde, Universidade Federal de Ciências da Saúde de Porto Alegre - UFCSPA.

**Julia Fontoura**
Departamento de Ciências Básicas da Saúde, Universidade Federal de Ciências da Saúde de Porto Alegre - UFCSPA.

**Priscila de Souza**
Departamento de Ciências Básicas da Saúde, Universidade Federal de Ciências da Saúde de Porto Alegre - UFCSPA.

**Gabriel Hilario**
Departamento de Ciências Básicas da Saúde, Universidade Federal de Ciências da Saúde de Porto Alegre - UFCSPA. https://orcid.org/0000-0001-5314-2131

**Renata Zorzetto**
Departamento de Ciências Básicas da Saúde, Universidade Federal de Ciências da Saúde de Porto Alegre - UFCSPA. https://orcid.org/0000-0003-3105-1014

**Luiz Rodrigues Júnior**
Departamento de Ciências Básicas da Saúde, Universidade Federal de Ciências da Saúde de Porto Alegre - UFCSPA.

**Veridiane Pscheidt**
Departamento de Ciências Básicas da Saúde, Universidade Federal de Ciências da Saúde de Porto Alegre - UFCSPA.

**Jayme Ferreira Neto**
Departamento de Ciências Básicas da Saúde, Universidade Federal de Ciências da Saúde de Porto Alegre - UFCSPA.

**Alisson Haubert**
Departamento de Ciências Básicas da Saúde, Universidade Federal de Ciências da Saúde de Porto Alegre - UFCSPA.

**Izza Gambin**
Departamento de Ciências Básicas da Saúde, Universidade Federal de Ciências da Saúde de Porto Alegre - UFCSPA.

**Aline Oliveira**
Departamento de Ciências Básicas da Saúde, Universidade Federal de Ciências da Saúde de Porto Alegre - UFCSPA.
**Raissa Mello**
Departamento de Ciências Básicas da Saúde, Universidade Federal de Ciências da Saúde de Porto Alegre - UFCSPA.
**Matheus Balbe e Gutierres**
Departamento de Ciências Básicas da Saúde, Universidade Federal de Ciências da Saúde de Porto Alegre - UFCSPA.
**Rodrigo Gassen**
Center for Transplantation Sciences, Department of Surgery, Massachusetts General Hospital, Harvard Medical School
**Ivaine Sartor**
Social responsibility – PROADI-SUS, Hospital Moinhos de Vento
**Gabriela Zavaglia**
Social responsibility - PROADI-SUS, Hospital Moinhos de Vento https://orcid.org/0000-0001-5419-665X
**Ingrid Fernandes**
Social responsibility – PROADI-SUS, Hospital Moinhos de Vento
**Fernanda Varela**
Social responsibility – PROADI-SUS, Hospital Moinhos de Vento
**Márcia Polese-Bonatto**
Social responsibility – PROADI-SUS, Hospital Moinhos de Vento
**Thiago Borges**
PUCRS
**Sidia Callegari-Jacques**
Departamento de Estatística, Universidade Federal do Rio Grande do Sul
**Marcela da Costa**
Coordenação-Geral do Programa Nacional de Imunizações – Departamento de Imunizações e Doenças Transmissíveis – Secretaria de Vig
**Jaqueline Schwartz**
Coordenação-Geral do Programa Nacional de Imunizações – Departamento de Imunizações e Doenças Transmissíveis – Secretaria de Vig
**Marcelo Scotta**
Social responsibility – PROADI-SUS, Hospital Moinhos de Vento
**Renato T. Stein Stein**
Social responsibility – PROADI-SUS, Hospital Moinhos de Vento
**Cristina Bonorino** ( cristinabonorino@gmail.com )

Universidade Federal de Ciências da Saúde de Porto Alegre - UFCSPA https://orcid.org/0000-0003-2755-3978

**Article**

**Keywords:** COVID-19, SARS-CoV-2, pediatrics, anti-viral responses

**Posted Date:** May 7th, 2021

**DOI:** https://doi.org/10.21203/rs.3.rs-424079/v1



**Version of Record:** A version of this preprint was published at Nature Communications on November 25th, 2021. See the published version at https://doi.org/10.1038/s41467-021-27120-y.

# Strong specific anti-viral responses in pediatric COVID-19 patients in South Brazil


## Authors

Tiago Fazolo[1*], Karina Lima[1*], Julia C. Fontoura[1*], Priscila Oliveira de Souza[1], Gabriel Hilario[1], Renata Zorzetto[1], Luiz Rodrigues Júnior[1], Veridiane Maria Pscheidt[1], Jayme de Castilhos Ferreira Neto[1], Alisson.F. Haubert[1], Izza Gambin[1], Aline C. Oliveira[1], Raissa S. Mello[1], Matheus de Bastos Balbe e Gutierres[1], Rodrigo Benedetti Gassen[5], Ivaine Tais Sauthier Sartor[3], Gabriela Oliveira Zavaglia[3], Ingrid Rodrigues Fernandes[3], Fernanda Hammes Varela[3,4], Márcia Polese-Bonatto[3], Thiago J. Borges[5], Sidia Maria Callegari-Jacques[6], Marcela Santos Correa da Costa[7], Jaqueline de Araujo Schwartz[7], Marcelo Comerlato Scotta[3,4], Renato T. Stein[3,4], Cristina Bonorino [1,2**]

## Affiliations

1. Departamento de Ciências Básicas da Saúde, Universidade Federal de Ciências da Saúde de Porto Alegre - UFCSPA. Porto Alegre RS Brazil
2. Department of Surgery, University of California at San Diego- UCSD. La Jolla, CA USA
3. Social Responsibility – PROADI-SUS, Hospital Moinhos de Vento, Porto Alegre, Brazil
4. Escola de Medicina, Pontifícia Universidade Católica do Rio Grande do Sul - PUCRS, Porto Alegre, Brazil
5. Center for Transplantation Sciences, Department of Surgery, Massachusetts General Hospital, Harvard Medical School, Boston, MA
6. Departamento de Estatística, Universidade Federal do Rio Grande do Sul

7. Coordenação-Geral do Programa Nacional de Imunizações, Departamento de Imunizações e doenças transmissíveis, Secretaria de vigilância em saúde - Ministério da Saúde (CGPNI/DEIDT/SVS/MS)

*, equally contributed to this work; **, corresponding author

## Abstract

Epidemiological evidence that COVID-19 manifests as a milder disease in children compared to adults has been reported by numerous studies, but the mechanisms underlying this phenomenon have not been characterized. It is still unclear how frequently children get infected, and/or generate immune responses to SARS-CoV-2. We have performed immune profiling of pediatric and adult COVID-19 patients in Brazil, producing over 38 thousand data points, asking if cellular or humoral immune responses could help explain milder disease in children. In this study, pediatric COVID-19 patients presented high viral titers. Though their non-specific immune profile was dominated by naive, non-activated lymphocytes, their dendritic cells expressed high levels of HLA-DR and were low in CX3CR1, indicating competence to generate immune responses that are not targeted to inflamed tissue. Finally, children formed strong specific antibody and T cell responses for viral structural proteins. Children's T cell responses differed from adults in that their CD8+ TNFα+ T cell responses were low for S peptide but significantly higher against N and M peptide pools. Altogether, our data support a scenario in which SARS-CoV-2 infected children may contribute to transmission, though generating strong and differential responses to the virus that might associate with protection in pediatric COVID-19 presentation.

## Introduction

COVID-19 is a complex disease, with multisystemic involvement, and an array of clinical manifestations that can vary from asymptomatic to severe outcomes leading to death (1) which lead to an ongoing worldwide emergency (2). Epidemiological evidence of less severe forms of the disease and reduced mortality in children upon infection with SARS-CoV-2 has been consistently reported (3,4), except for an inflammatory syndrome (MISC) associated with co-morbidities in a relatively low percentage of children (5). The pediatric population (0-19 years old) represents more than 25% of the Brazilian population, however, it is observed that this group corresponds to only 1.9% (19,589 / 989,170) of all cases of SARS by COVID-19 reported in the past 12 months. Mortality among children represented 0.5% (1,564 / 321,659) of all deaths due to the disease reported in the same period. The lethality in children and adolescents hospitalized due to SARS by covid-19 was 8.0% (1,574 / 19,589), while the overall lethality in all age groups was 32.5% (321,659 / 989,170), in the observed period (data from SIVEP-Gripe, Brazilian Ministry of Health). Thus, a significantly lower number of children and adolescents has severe clinical presentations with the need for hospitalization, or that will lead to death, when compared to other age groups.

Different hypotheses have been raised to explain this phenomenon (6,7). Milder disease in children could result from a reduced expression of the viral receptor ACE2, leading to lower levels of viral replication (8). Alternatively, it could be explained by a differential immune response in children, correlated to a distinct infection course from adults (9). A third popular hypothesis is that the pre-existence of neutralizing antibodies to seasonal coronaviruses could confer some cross-protection against SARS-CoV-2 induced disease, mainly because children are considered the main reservoir for these viruses (10). At present, the scarcity of data prevents

a clear understanding of the striking differences between the pediatric and adult outcomes after infection by COVID-19.

Comprehensive studies have characterized immune responses in adults with mild or severe forms of COVID-19 (11–14). However, considerably fewer studies have focused on pediatric patients. This is a subject of paramount importance, not only because it is central to the design of public policies regulating school opening (and all the activities associated with it) during the pandemic, but also because understanding the milder disease presentation in children may provide important clues for the design of prevention strategies as well as novel therapeutic pathways for the management of COVID-19. In this study, we sought to characterize in detail the innate and adaptive immune responses in a cohort of patients consisting of children with mild disease and adults with different degrees of severity presenting at health care facilities with symptoms suggestive of COVID-19. We sought to identify an immune profile in children that could explain the striking differences in outcome between them and adult COVID-19 patients. We collected plasma and peripheral blood mononuclear cells (PBMCs) from adult and pediatric COVID-19 patients, and detailed characterization of their immune response was performed by multi-parameter flow cytometry, defining 78 immune cell subsets and expression of key activation markers, anti-SARS-CoV-2 IgA and IgG antibodies, and frequencies of specific effector T cells, producing 38,670 data points. Pediatric patients with mild COVID-19 had high viral load titers, high frequencies of dendritic cells, with high HLA-DR expression, but low in CX3CR1. Although their non-specific adaptive cells immune profile was dominated by antigen-inexperienced cells, SARS-CoV-2 specific antibodies and T cells were detected in levels comparable to the ones in adults with either severe or mild disease. Children showed higher CD8+ TNFα+ T cell responses to N and M peptide pools than for S peptides, while this was not observed in adults. This response did not correlate with anti-S or anti-N antibody levels. Taken together, our findings suggest that children produce a differential immune

response when compared to adults, which associates with the mild manifestation in pediatric COVID-19.

## Methods

### Ethics Statement

This study was approved by the Institutional Review Board (IRB 30749720.4.1001.5330) at Hospital Moinhos de Vento and by the Ethics Committee at Universidade Federal de Ciências da Saúde (CAAE 30749720.4.3001.5345). Legal consent was obtained from all participants or their legal guardians. The study was conducted according to good laboratory practices and following the Declaration of Helsinki.

### Patients

A prospective cohort study was carried out at Hospital Moinhos de Vento and at Hospital Restinga e Extremo Sul, both in Porto Alegre, southern Brazil. A convenience sample of adults and children older than 2 months were enrolled from June to December 2020 at either the outpatient clinics (OPC), emergency rooms (ER), or hospitalized. Subjects were screened if presenting cough and/or axillary temperature ≥37.8ºC and/or sore throat. Both blood samples and respiratory samples collected through nasopharyngeal swabs were obtained at enrollment. Only patients with the clinical diagnosis of COVID-19 and SARS-CoV-2 infection confirmed by RT-PCR were included in the study. Clinical and demographic data were collected at inclusion, following a standardized protocol. Disease severity was classified according to the World Health Organization classification after completing the follow-up questionnaire (15).

SARS-CoV-2 RT-q-PCR

A qualitative RT-PCR assay to SARS-CoV-2 was performed for all participants. Bilateral nasopharyngeal and oropharyngeal swabs were collected and placed in the same transport medium with saline solution and RNAlater®, RNA Stabilization Solution (Catalog number AM7021, Invitrogen™). MagMax™ Viral/Pathogenic Nucleic Acid Isolation Kit (Applied Biosystems) was used to extract viral RNA in the KingFisher Duo Prime System (ThermoFisher, USA) automated platform. The RT-PCR assay was performed in 10 µL total reaction, using Path™ 1-Step RT-qPCR Master Mix, CG (catalog number A15299, AppliedBiosystems) and TaqMan™ 2019-nCoV Assay Kit v1 (catalog number A47532, AppliedBiosystems) which comprises the SARS-CoV-2–specific targets (gene ORF1ab, gene S and gene N). As reaction control was used 5 µL (200 copies/µL) the TaqMan™ 2019-nCoV Control Kit v1 (catalog number A47533, AppliedBiosystems). QuantStudio 5 (ThermoFisher Scientific, USA) was used to perform the PCR.

PBMC isolation and cryopreservation

Blood was collected in EDTA tubes (Firstlab, PR, Brazil) and stored at room temperature before processing for PBMC isolation and plasma collection. Plasma was separated by centrifugation and cryopreserved. PBMCs were next isolated by density-gradient centrifugation using Ficoll–Paque™ PLUS (GE Healthcare®), and either studied directly or resuspended in FBS 5% DMSO and stored in liquid nitrogen until use.

Flow cytometry

Cells were thawed by diluting them in 5mL pre-warmed complete RPMI1640 medium (Sigma-Aldrich - R8758) containing 5% FBS and spun at 1500 rpm for 5 minutes. Supernatants were carefully removed, and cells were resuspended in PBS. After, were stained with the BD Horizon™ Fixable Viability Stain 510 together with antibodies for surface markers, as follows: anti-CD3-APC-H7 (clone SK7), anti-CD24-APC-H7 (clone ML5), anti-HLA-DR-APC-H7 (clone G46-6), anti-CD4-PerCP-Cy5.5 (clone RPA-T4), anti-CD27-PerCP-Cy5.5 (clone M-T271), anti-CD11c-PerCP-Cy5.5 (clone B-ly6), anti-CD14-PerCP-Cy5.5 (clone M5E2), anti-CD8-FITC (clone HIT8a), anti-IgG-FITC (clone G18-145), Lineage 2-FITC (cat. 643397), anti-CD16-FITC (clone 3G8), anti-CXCR5 (CD185)-BB515 (clone RF8B2), anti-CD19-APC (clone HIB19), anti-CD127-Alexa 647 (clone HIL-7R-M21), anti-CX3CR1-Alexa647 (clone 2A9-1), anti-CD69-APC (clone FN50), anti-CD38-PE (clone HIT2), anti-ICOS (CD278)-PE (clone DX29), anti-CD141-PE (clone 1A4), anti-CD66b-PE (clone G10F5), anti-CD137 (4-1BB)-PE (clone 4B4-1), anti-HLA-DR-PE-Cy7 (clone G46-6), anti-CD19-PE-Cy7 (clone SJ25C1), anti-CD25-PE-Cy7 (clone 2A3), anti-CD45RA-PE-Cy7 (clone L48), anti-IgM-BV421 (clone G20-127), anti-PD-1 (CD279)-BV421 (clone MIH4), anti-CD303-BV421 (clone V24-785), anti-CD56-BV421 (clone NCAM 16), anti-CCR7-BV421 (clone 2-L1-A) antibodies. For intracellular staining, cells were first stained for surface markers and subsequently fixed and permeabilized using the Transcription Factor Buffer Set (BD Biosciences-Pharmingen, USA), then stained with anti-Ki-67-BV421 (clone B56), anti-Perforin-Alexa 647 (clone δG9), and anti-Granzyme B-BV421 (clone GB11) antibodies. Following *in vitro* stimulation assays with specific peptides, cells were stained with the BD Horizon™ Fixable Viability Stain 510 and anti-CD3-PE-Cy7 (clone SK7), anti-CD4-PerCP-Cy5.5 (clone RPA-T4), anti-CD8-APC-H7 (clone SK1), anti-CCR7-BV421 (clone 2-L1-A),

and subsequently fixed and permeabilized using the Cytofix/Cytoperm kit (BD Biosciences-Pharmingen, USA), then stained with anti-IFNγ-FITC (clone 4S.B3), anti-TNF (clone MAb11) and anti-IL-17-PE (clone SCPL1362) antibodies. All samples were analyzed using a BD Biosciences - FACSCanto II and FlowJo 10.7.1 software.

*In vitro* T cells stimulation assays

PBMC were thawed, assayed for viability, counted, and plated in 96-well plates at $3\times10^6$ PBMCs/mL, 100 uL/well in RPMI1640 medium (Sigma-Aldrich - R8758) supplemented with 10% fetal bovine serum (100 IU of penicillin/mL, 100 μg of streptomycin/mL (Lonza, Belgium) and 2 mM L-glutamine (Lonza, Belgium) (R10H medium), and subsequently stimulated with peptide PepTivator SARS-CoV-2 Prot S (130-126-700 - Miltenyi Biotec, Germany), PepTivator SARS-CoV-2 Prot N (130-126-698 - Miltenyi Biotec, Germany) and PepTivator SARS-CoV-2 Prot M (130-126-702 - Miltenyi Biotec, Germany) at 1 μg/mL. PMA (50 ng/mL, Sigma, USA) plus ionomycin (1 μg/mL, Cayman chemical company, USA) and DMSO were used as positive and negative controls for stimulation, respectively. Stimulation with a CMV peptide pool at 2μg/mL (Mabtech, Sweden) was also performed, as a positive control for the assay. All treatments were submitted for 18h at 37ºC and 5% $CO_2$. Three hours before harvesting, Golgi Plug (BD Biosciences, USA) 1μg/mL was added to each well. Cells were stained and analyzed for phenotype as described above.

ELISA

Plasma was tested for IgG and IgA antibodies to S-RBD protein (#RP-87678 - Invitrogen, USA) and N protein (kindly provided by Dr. Ricardo Gazinelli - Fiocruz Belo Horizonte,

Brazil) using a protocol described in (16). Briefly, ELISA plates (Kasvi, Brazil) were coated overnight with 1μg/mL of SARS-CoV-2 Spike Protein (S-RBD). On the following day, plates were blocked for 1 h at room temperature with blocking buffer (3% Skim Milk Powder in Phosphate Buffered Saline (PBS) containing 0.05% Tween-20). Plasma samples were heat-inactivated at 56°C for 60 minutes and then serially diluted in 1% milk in 0.05% PBS-Tween 20 starting at a 1:25. Plasma was incubated for 2 h at 37°C. Secondary antibodies were diluted in 0.05% PBS-Tween and incubated for 1 h at room temperature. For both IgG, anti-human peroxidase produced in rabbit (#IC-1H01 - Rhea Biotec, Brazil), and IgA, anti-human peroxidase produced in goat (#A18781 - Invitrogen, USA), was used at a 1:10,000 dilution. The assay was developed with TMB Elisa Substrate - High Sensitivity (Abcam, United Kingdom) for 30 minutes, and the reaction stopped with 1M chloric acid. Readings were performed in an ELISA reader (Biochrom EZ 400), and O.D. at 450 nm was used to calculate the area under the curve (AUC), using a baseline of 0.07 for peak calculation (17).

Statistics

Percentages were used to describe categorical variables. Pearson's Chi-square test was used to evaluate proportions among the children, severe and mild adults. Data normality assumptions were verified for continuous variables and summarized in terms of median and interquartile range (IQR). Two-tailed Kruskal-Wallis test followed by Benjamini-Hochberg correction for multiple comparisons was used to compare values among the groups. Principal Component Analysis (PCA) was employed to reduce the dimensions of 78 immunological variables generated by flow cytometry analysis, to explain the total variability with a smaller, new set of variables. Spearman correlations were performed between all variables (every set of two variables) and within sets of variables to identify clusters of correlated variables. In PCA of the

variables grouped in clusters, variables containing redundant information were excluded. Comparison among groups regarding single variables or PC values was performed by non-parametric Kruskal-Wallis test, followed by 2 by 2 multiple comparisons with p-values adjusted accordingly. All analyses were performed either in GraphPad Prism v.9 or R and sometimes confirmed in Python. 3D analysis of PCA was plotted in Python. Scripts are detailed in supplemental materials.

## Results

The study design is summarized in Figure 1A. We have recruited a total of 92 patients (25 children; 34 adults with mild disease - AMD; and 33 adults with severe disease - ASD). All subjects had COVID-19 confirmed by PCR. All children had mild disease and were treated as outpatients. Their characteristics are described in Table 1. The youngest individual enrolled was 7 months old – which does not appear in the table because only the interquartile interval (IQR) is shown. Most individuals were Caucasian. As expected, comorbidities were concentrated in the group with severe disease, which was also the group with a higher mean age. Some symptoms are probably not accurately assessed in some children, such as anosmia or dysgeusia, due to the age of some individuals in this group. Dyspnea was significantly less frequent in children. Median Ct levels for all three probes used in PCR were higher in AMD, and not different between ASD and children.

### Immune responses separate pediatric patients, adults with mild and severe disease from each other

Comprehensive immune profiling of PBMCs from pediatric and adult patients was performed using flow cytometry, generating 78 variables (frequencies of cell subpopulations and gMFI of activation markers). Gating strategies are detailed in Supplementary Figure 1 (A-H). To reduce the dimensionality of the numerous variables, a PCA analysis was carried out. This approach indicated that the three groups (pediatric patients; mild adult patients -AMD; and severe adult patients - ASD) separated from each other based on three of the new variables created, PC1, PC2, and PC3. PC1 separated the three groups, while PC2 separated mild patients from severe ones (Figure 1B). 3D plotting performed to include PC3 showed that children again separated from mild and severe adult patients (Figure 1C) and confirmed in 2D (Figure 1D). The PC scores from all three groups were plotted and the significance of these differences was analyzed by a Kruskal-Wallis (KW) test. Children had the highest mean score value for PC1 (2.765), followed by AMD (0.142) and ASD (-2.351), and these differences were highly significant (Figure 1E). For PC2, AMD had a mean score of 2.079, higher ($p<0.0001$) from children and ASD (mean scores of -1.585 and -1.180, respectively, $p>0.999$). PC3 scores were highest in children (mean=1.384) and significantly different from adults with mild (mean=-0.629; $p<0.0047$) and severe (mean=-0.247; $p<0.0181$) disease.

Principal components are calculated based on correlations among variables, and to interpret the meaning of each PC we analyzed the positive or negative contributions (loadings) of each variable in each PC. The variables with the main positive and negative contributions (loadings) are identified in Figures 1F, for PC1 and PC2; and 1G, for PC3. Respective loadings values are listed in Supplementary Table 1. PC1 had positive inputs mainly by IgM+ memory B cells, naïve B cells, and cDC1 DR expression; and main negative contributions by proliferating B cells; plasmablasts; and CX3CR1+ expression in dendritic cells (DC) (Figure 1F). That indicated that the group with the highest mean scores for PC1 (children) would be characterized by a profile of predominantly naive or low-affinity memory B cells, not

activated/differentiated; and their dendritic cells would be high in DR, but low in CX3CR1. The opposite would be true for individuals with the lowest mean scores (ASD), while AMD would be characterized by an intermediate profile for these variables. The main positive influences for PC2 were T regs, mDCs, and TEMRA cells, indicating mild adult patients present significantly higher frequencies of these cell subpopulations. The main negative influences for PC2 were eosinophils, NK cells, and granulocytes (Figure 1F), and these should be the lowest in AMD. For PC3 (Figure 1G), the main positive contributions came from naive CD8+ T cells, naive CD4+ T cells, and pDCs; and main negative contributions were DCs; and expression of HLA-DR in mDC and cDC1. Because children had the highest scores for PC3, they should have significantly higher frequencies of such cells (and higher expression of HLA-DR in DCs) compared to both AMD and ASD. To verify these PCA interpretations, we compared them to the analysis of variance (Kruskal-Wallis) results performed among the three groups of patients regarding the three most relevant, positive (Figure 2A) and negative (Figure 2B) influencers, variables for PC1, PC2, and PC3. The comparison of the three groups for their variances regarding each variable agreed with the differences among them detected by PCA. A pattern that emerged from these two combined analyses was that children, AMD and ASD, separate from each other based mostly on differences in the state of activation of B and T lymphocytes, and in targeting innate inflammatory responses to inflamed tissues.

The percent of the total variability explained by these first principal components was low; the first three PCs together explained only 28.81% of the variance (Supplementary Table 1). This indicated that these 78 variables were not highly correlated as a whole. A correlation analysis using Spearman´s coefficient confirmed this observation (Supplementary Figure 2), revealing a general pattern of moderate to weak correlations, but also identifying clusters of variables that were more correlated than others. These clusters represented six types of immune "signatures": Proliferating/activated T cells; DCs; Granulocytes + Monocytes; NK cells; B

298 cells; and memory T cells. Follicular helper T cells (Tfh) related variables were weakly
299 correlated and were not considered as a cluster. We thus performed six separated PCAs for the
300 identified clusters of variables, hypothesizing that they could bring more specific information
301 to explain immunological differences among the three groups of patients. In this analysis, the
302 first two PCs for each cluster were now explained a larger portion of the total variance (44.19,
303 63.17, 50.37, 67.35, 49.56, and 42.49%, respectively - Supplementary Table 1) among the three
304 types of patients, and their distributions in children, AMD and ASD were analyzed. The results
305 are shown in Figure 3 (A-D) and Supplementary Figure 3 (A-C), with the respective graphic
306 representations for scores and loadings. We started by analyzing PCs formed by the innate
307 cells' signatures. Principal components for the clusters of Granulocytes + Monocytes (Figure
308 3A) and NK cells (Figure 3B), although derived from expressive correlations among their
309 respective variables, did not separate the three groups of patients, indicating that the individuals
310 were not significantly different for the variables that composed these PCs. That was intriguing
311 because those variables had, as stated above, important contributions for the PC2 of all
312 variables (Figure 1), but it also indicated that this contribution helped separate the groups
313 mostly based on their correlations with other variables in the group of all variables, and not on
314 the differences among groups for those variables alone. Although highly correlated among
315 them (Supplementary Figure 2), variables composing the signatures for Granulocytes +
316 Monocytes and NK cells did not separate the groups when used together in a PCA (not shown)
317 and did not generate any new information.
318 Findings in PCA for the DCs signature (Figure 3C) indicated that children were significantly
319 separated from ASD, but not from AMD, with lower scores for PC1 (mostly CX3CR1
320 expression in DCs) and higher scores for frequencies of DCs (Figure 3C). HLA-DR expression
321 in DCs subpopulations constituted negative contributions for PC1. This indicated that children,
322 as well as AMD, would have more DCs than ASD, high in HLA-DR and low in CX3CR1. That

was confirmed by the KW analysis of the three groups (Figure 3C). Spearman correlation analysis (Figure 3D) evidenced that CX3CR1 expression was negatively correlated with HLA-DR expression. These results suggested that high DCs frequencies in blood, with low CX3CR1, but high HLA-DR expression could be involved, or at least serve as markers, for mild disease. Inversely, low DCs frequencies, with high CX3CR1 expression, could be associated with more severe disease.

PCA for the clusters involving adaptive cells variables was performed next and are shown in Supplementary Figure 3. B cells (Supplementary Figure 3A, Supplementary Table 1) and T cell activation/proliferation (Supplementary Figure 3B, Supplementary Table 1) PCA corroborated a general pattern of response in children, either separating from the other groups (only sometimes grouping with AMD, apart from ASD). KW analysis of mean scores for each PC showed that in some cases children presented some significant differences from AMD. For example, PC1 of B cells recapitulated findings from the first analysis, mainly positively influenced for IgM+ B cells and naive cells, and showed children with significantly higher scores, compared to mild and ASD ($p<0.01$). Children were grouped with AMD ($p=0.1599$), and apart from ASD ($p<0.0001$), regarding PC1 of T cell activation/proliferation (Supplementary Figure 3B). The ASD had the highest scores for this PC, highly influenced by activated and proliferating CD4+ and CD8+ T cells, suggesting that adults with severe disease were characterized by higher frequencies of activated, Ki67+ T cells, and the opposite would be observed for children and AMD – though this was not always corroborated by the KW analysis. Finally, PCA for T cell memory clustered variables showed a trend to separate the three groups (Supplementary Figure 3C). PC1 scores, strongly positively influenced by naive T cells, but negatively influenced by effector memory T cells (TEM), significantly separated children from AMD ($p=0.0005$), and these somewhat separated from ASD ($p=0.0410$), indicating children and AMD would have lower frequencies of TEM and higher frequencies of

naive T cells compared to ASD. Terminally differentiated memory CD4+ and CD8+ T cells (TEMRA) were strong positive influences for PC2, while expression of CD69 and CD137 in TEM cells negatively influenced PC2. Children and AMD, with high scores for PC2, did not differ from each other, suggesting they would both be characterized by higher frequencies of TEMRA (especially CD4+ TEMRA) cells than ASD, which in turn would have higher frequencies of activated, CD69+, CD137+, TEM cells. Confirmations of the interpretations of these PCs were again sought in the KW analysis for individual variables next to each PCA results (Supplementary Figure 3C), and also in Supplementary Figure 4 - which compiles all the remaining variables KW analyses results. This led us to note that for TEMRA, children differed from AMD and not from ASD. CD45RA, a marker upregulated both in naïve and TEMRA cells, has been shown to show different expression during the generation of memory pools of chronic infections (18) as well as in response to vaccination (19). CD4+ TEMRA cells associated with protection in Dengue (20). Thus, the PCA could indicate possible differences for children and AMD, compared to ASD, in pathways for the generation of memory. In the KW comparisons, CD4+TEMRA cells were lower in children than in AMD, and only AMD differed from ASD significantly. For TCM, there were no differences among groups (Supplementary Figure 4). Altogether, the patterns revealed by PCA indicated that children have higher frequencies of non-specific antigen inexperienced B and T cells and DCs, with high HLA-DR and low CX3CR1 expression. In some cases, children and AMD shared not only a mild presentation of the disease but also a similar immune profile. Finally, the immune profile of ASD was characterized by higher frequencies and markers of T and B cell activation and proliferation, TEM cells, and lower DCs with high expression of CX3CR1.

SARS-CoV-2 specific T cells and antibodies responses in children are comparable to the ones of adult patients

The characteristics of the non-specific immune profile of children led us to ask if they had effectively formed SARS-CoV-2 specific responses upon infection. Seroconversion after infection with SARS-CoV-2 patients with all forms of the disease has been described by several studies - reviewed in (21). Antibodies to the S protein, and more specifically to the RBD of this protein, are clinically considered a hallmark of infection, and frequently proposed as a correlate of protection. We thus compared children, AMD, and ASD for their RBD specific- IgA and IgG titers. On average, children presented levels of both IgG and IgA comparable to the adult patients (Figure 4). In our cohort, although some individuals from the ASD group presented higher levels of antibodies, differences among the groups were non-significant. Our results revealed that, even though children presented a generally naive, non-activated, immune profile, they had efficiently generated SARS-CoV-2 specific antibody responses, in levels that did not differ from the ones in AMD ($p<0.103$ for IgA; $p>0.999$ for IgG) or ASD ($p<0.916$ for IgA; $p>0.999$ for IgG) COVID-19 patients.

We next asked if children had generated specific effector T cell responses to SARS-CoV-2. There are four structural proteins in SARS-CoV-2: the spike glycoprotein (S), the envelope (E) protein, the membrane (M) protein, and the nucleocapsid (N) protein. Specific effector T cell responses have been described in adult COVID-19 patients, both with mild and severe disease (22,23), however fewer studies have focused on specific immune responses in pediatric patients infected with SARS-CoV-2. We measured the frequencies of CD4+T and CD8+T cells expressing TNF$\alpha$, IFN$\gamma$, or IL-17 in response to stimulation by peptide pools of the S, N, and M proteins of the virus (Figure 5). Figure 5A shows representative flow cytometry plots of cytokine-producing CD4+ or CD8+ T cells upon stimulation with SARS-CoV-2 peptide pools. Negative (DMSO) and positive (PMA + ionomycin) control representative plots can be seen in Supplementary Figure 5. Children presented detectable CD4+ and CD8+ T cell responses upon stimulation with all three peptide pools (Figure 5B). When we compared types of

responses in each group for the different peptide pools, children showed a significantly higher CD8+T TNFα+ response for the M ($p<0.005$) and for the N ($p<0.0409$) peptide pools than for the S pool (5B, upper right panel). This was not seen in adults, and although there was a trend for lower CD4+ TNFα+ responses in children, it was not significant. Supplementary Figure 6 shows the responses compared among the groups. About 30% of individuals – of all groups - did not show responding CD4+ T cells to the peptide pools; a higher frequency of individuals did not respond to the S pool compared to the M and N pools. In the ones that responded, CD4+ IL-17+ T cell responses were higher for all three peptide pools (about 1 log higher than INFγ and TNFα CD4+T cell responses). CD8+ T cell responses were, in general, more robust, although for S and M peptide pools there were still some individuals, though fewer, that did not respond to stimulation. The absence of response, in our sample, did not correlate with the early time of collection, as reported by (18). TNFα+ CD8+ T cell responses were about 1 log higher than what was detected for CD4+ T cells, for all peptide pools (Supplementary Figure 6). The IL-17+ CD4+T cells responses to stimulation by all three pools, were higher than the TNFα+CD4+ and INFγ+ CD4+ for all three groups. The differential TNFα+ cytotoxic response to M and N peptides seen in children led us to investigate levels of anti-N antibodies. Children made strong anti-N IgG levels, not different from AMD and ASD (Figure 6A). Anti-RBD IgA, but not IgG levels, correlated positively with CD4+ INFγ+ responses (Figure 6B). Interestingly, the TNFα+ cytotoxic responses to M and N peptide pools were inversely correlated with levels of anti-RBD and anti-N antibodies (Figure 6B). Anti-N antibody levels correlated positively with anti-N CD4+INFγ+ responses (Figure 6B). Taken together, these results indicate that children do generate specific humoral and effector cell responses upon infection with SARS-CoV-2, with a differential, higher cytotoxic response against proteins M and N, not associated with antibody responses to the spike protein.

## Discussion

It is clear from our study as well as from others (24) children do get infected by SARS-CoV-2, and thus possibly contribute to the community-based spread of the virus, contrary to what has been suggested by studies on the low nasal ACE2 expression in children (25). The lower rates of infection in children can be biased by lower testing, as suggested by (26), and should be more carefully studied, given its importance for planning school openings. Our findings on the more naïve, non-specific lymphocyte profile presented by in children, if taken isolated from the other results in this study, could indicate that a naive immune system does better than an old one, as has been suggested (9) – that children would be better equipped to mount fast and efficient immune responses to rapidly clear the virus. However, one prediction from this hypothesis is that children would be more likely to present mild forms of all viral diseases, and this is not the case. While milder manifestations are observed in MERS, SARS, and varicella, the opposite is observed for infection with poliovirus, and also respiratory viruses, especially influenza and respiratory syncytial virus (RSV) - reviewed in (6).

Our data indicate the possibility that not only the adaptive but also their innate immune system has relevant characteristics that enabled children to mount an efficient immune response and control the infection. The important differences observed for dendritic cells might offer an important clue. DCs play crucial roles in initiating and shaping the adaptive response, and subpopulations of DCs, especially pDC, are determinants for the generation of efficient antiviral responses, being one of the main sources of type I interferon (27). A previous study in COVID-19 adult patients indicated decreased activation and numbers of DCs (28). In our study, children consistently showed higher frequencies of DCs, including pDCs, compared to adults. High HLA-DR expression is characteristic of mature DCs; as they become activated by engagement of pattern recognizing receptors, HLA-DR first increases, and then decreases as

448 DCs migrate to draining lymph nodes (27,29) Low HLA-DR expression in children is
449 associated with immune suppression (4) and acute inflammatory conditions (30). The inverse
450 correlation of HLA-DR with CX3CR1 in DCs is intriguing. CX3CR1, also known as the
451 fractalkine receptor, is considered a homing marker for inflamed tissue and plays a role in
452 pathology in Japanese virus-induced encephalitis ref (31) and peritoneal vasculitis in a sepsis
453 model (32). The high levels of HLA-DR in children's DCs indicate that their cells are not
454 poorly activated, but mature and able to generate efficient immune responses. The low
455 expression of CX3CR1 suggests that children's DCs are not targeted to inflamed sites, as they
456 seem to be in ASD. Our results indicate that expression of CX3CR1 in circulating DCs could
457 associate, or serve as a marker for, pathological mechanisms in severe COVID-19, and suggest
458 that inflammation to specific sites such as the lung may be affected by age.
459 Pediatric patients in our sample presented SARS-CoV-2- specific antibodies and T cell
460 responses in levels comparable to adult patients. Based on our data, we propose that the higher
461 CD8+TNFα+ responses for the M and N proteins could be associated with a protective
462 response in children. The M protein is the most abundant structural protein on the surface of
463 the virus (33), thus it could potentially constitute an important target of immune responses. A
464 study by Thieme et al. (34) found anti-M CD4+ T cells as the highest T cell response in critical
465 COVID-19 patients. In that study, CD4+ T, rather than CD8+ T cell immunity to SARS-CoV-
466 2 proteins dominated the response in severe and critical patients, indicating that a robust CD4+
467 T cell response to these antigens was not determinant for protection. The nucleocapsid (N)
468 protein is structural, and though not expressed on the surface, abundantly produced upon
469 infection, and highly conserved among beta coronaviruses (35). This protein was a major target
470 for early B cell responses in the SARS epidemic of 2003 (36). More recent studies (17,37)
471 found strong T cell responses to the N protein in SARS-CoV-2 patients, and also in individuals
472 who recovered from SARS. These studies support a relevant role for structural N protein as an

473 immune target in SARS-CoV-2 infection. We found robust antibody responses in children both
474 to the S RBD as well as to the N protein, while Weisberg et al. (9) found antibodies to the S,
475 but not the N protein; and Cohen et al. (38) found lower responses in children in general. These
476 differences, as well as a lower response to the S protein in general in our sample, may reflect
477 differences in HLA between American and Brazilian populations, or even a difference in
478 immunization history, given a tradition in vaccination program for children in Brazil. The
479 correlations of antibody responses with CD4+ T cells are somewhat expected, given the help
480 needed for antibody production, and indicate that these responses are somewhat coordinated,
481 but also that not all antibodies produced are linked to TNFα or INFγ help. Our next studies will
482 focus on further characterizing this antibody response in detail. The inverse correlation between
483 specific CD8+ T cell responses and antibodies may indicate a relevant role for cytotoxic
484 immunity against SARS-CoV-2, beyond antibody production.
485 Children are considered the natural reservoir of seasonal coronaviruses that cause the common
486 cold (4). A hypothesis frequently raised to explain milder disease in children with COVID-19
487 is that the presence of neutralizing antibodies to such viruses could cross-protect them upon
488 infection with SARS-CoV-2. However, a recent study in adults found no evidence of cross-
489 protection associated with levels of these antibodies (39). Alternatively, protection could be
490 conferred not by cross-reactive antibodies, but rather by pre-existing N-protein-specific T cells.
491 Most studies - and most vaccines - have so far focused on protection against SARS-CoV-2
492 infection by antibodies to the spike protein. Both screen studies by Ferreti et al. and Ng et al.
493 indicated that T cell immunity to SARS-CoV-2 infected individuals includes many targets
494 outside the spike protein and that they are not conserved among coronaviruses that cause the
495 common cold. These findings are in agreement with the ones of the Le Bert study. Our results
496 support that the role of T cell responses to the N protein must be further investigated, with a
497 more detailed T cell epitope mapping. Such work might reveal additional correlates of

protection, and/or epitopes to add in the next generation of COVID-19 vaccines. A recent report (40) indicated that T cell immunity was not markedly affected, so far, by the emergence of new variants, supporting the study of T cell epitopes to be added to the next vaccines.

The main limitation of this study is that it is mostly an exploratory, descriptive one, and compares individuals in different age groups. We believe this was a valid approach given the magnitude of what is unknown at the moment. Usually, biomarkers in peripheral blood are only useful when highly correlated with outcomes. Yet, most studies that seek to understand how immune responses can correlate with protection compare adult s with mild and severe disease, and it is known that these are in different age groups. At present, the best age-matched controls for SARS-CoV-2 infected patients are still unknown. Certainly, the absence of a pre-pandemic healthy children control group is a limitation of this and all the other studies that focused on the general, non-specific immune profile of children with COVID-19. There is still much to be understood about immunological differences not only between pediatric and adult COVID-19 patients but also in other diseases. In this sense, we believe our work contributes significant information which was collected in a completely unbiased investigation - we did not know what differences or similarities to expect. At the time the project started, COVID-19 numbers in Brazil were still not high and the frequency of MISC patients or children with severe manifestations of the disease was still too low to include. Inclusion of patients was easiest in ASD because they were admitted to the hospital, thus their time of symptoms to sample collection is shorter compared to AMD and children. However, we do not think this was a major influence in the results - if so, differences would have been highest between ASD and AMD, and that was not the case. Finally, these results are based on a single point of collection and we still do not know how they will evolve into the memory responses that will be ultimately generated. The study on this cohort is still ongoing, with two more points of sample collection. We expect that further analysis of our data, as well as other studies', on

immune profile data and specific responses, will bring relevant information on the generation of immune memory in pediatric COVID-19.

**Acknowledgments**

Funding for this study was provided by PROADI - HMV, and the Ministry of Health; fellowships for Karina Lima, Julia Fontoura, Renato Stein, and Cristina Bonorino are from CNPq; fellowships for Gabriel Hilario, Priscila Oliveira, and Tiago Fazolo are from CAPES. TJB is a recipient of an American Heart Association fellowship grant. We wish to thank Drs. André Báfica, Daniel Mansur, Helder Nakaya, Leo Riella, Graham Pawelec and Steve Hedrick for critical readings of this manuscript. Finally, we wish to thank all the patients who accepted to enroll in the study and donate blood.

**Tables**

Table 1. Clinical characteristics of all patients in this study.

Supplementary Table 1. Principal Component Analysis (PCA) variances and loading.

**Figures**

Main figures

1. Experimental approach and differential immune profile of children, mild and adult patients by principal component analysis.
2. Analysis of variance of the main variables contributing to principal components.
3. Principal Component Analysis of innate cells immune signatures.
4. Antibody responses.
5. Specific T cell responses.
6. Anti-N IgG response and correlation of specific responses.

Supplementary figures

1. Gating strategies for the key cell populations.
2. Spearman correlation of all variables composing the immune profile.
3. Principal Component Analysis of adaptive cells immune signatures.
4. Analysis of variance (Kruskall-Wallis) of remaining immune variables.
5. Control gate strategies for flow cytometry analysis of specific T cell responses.
6. Comparison of specific T cell responses by effector T cell type among the groups.

References


1. Zhou F, Yu T, Du R, Fan G, Liu Y, Liu Z, et al. Clinical course and risk factors for mortality of adult inpatients with COVID-19 in Wuhan, China: a retrospective cohort study. Lancet. 2020;395(10229):1054–62.
2. World Health Organization. WHO Coronavirus (COVID-19) Dashboard [Internet]. Available from: https://covid19.who.int/
3. Bialek S, Boundy E, Bowen V, Chow N, Cohn A, Dowling N, et al. Severe Outcomes Among Patients with Coronavirus Disease 2019 (COVID-19) — United States, February 12–March 16, 2020. MMWR Morb Mortal Wkly Rep. 2020;69(12):343–6.
4. Zimmermann P, Curtis N. COVID-19 in Children, Pregnancy and Neonates: A Review of Epidemiologic and Clinical Features. Pediatr Infect Dis J. 2020;39(6):469–77.
5. Cheung EW, Zachariah P, Gorelik M, Boneparth A, Kernie SG, Orange JS, et al. Multisystem Inflammatory Syndrome Related to COVID-19 in Previously Healthy Children and Adolescents in New York City. JAMA - J Am Med Assoc. 2020;324(3):294–6.
6. Singh T, Heston SM, Langel SN, Blasi M, Hurst JH, Fouda GG, et al. Lessons from COVID-19 in Children: Key Hypotheses to Guide Preventative and Therapeutic Strategies. Clin Infect Dis. 2020;71(8):2006–13.
7. Zimmermann P, Curtis N. Why is COVID-19 less severe in children? A review of the proposed mechanisms underlying the age-related difference in severity of SARS-CoV-2 infections. Arch Dis Child. 2020;1–11.
8. Schouten LR, van Kaam AH, Kohse F, Veltkamp F, Bos LD, de Beer FM, et al. Age-dependent differences in pulmonary host responses in ARDS: a prospective observational cohort study. Ann Intensive Care. 2019;9(1).
9. Weisberg SP, Connors TJ, Zhu Y, Baldwin MR, Lin WH, Wontakal S, et al. Distinct

antibody responses to SARS-CoV-2 in children and adults across the COVID-19 clinical spectrum. Nat Immunol. 2021;22(1):25–31.

10. Ng KW, Faulkner N, Cornish GH, Rosa A, Harvey R, Hussain S, et al. Pre-existing and de novo humoral immunity to SARS-CoV-2 in humans. bioRxiv. 2020;1343(December):1339–43.

11. Grifoni A, Weiskopf D, Ramirez SI, Mateus J, Dan JM, Moderbacher CR, et al. Targets of T Cell Responses to SARS-CoV-2 Coronavirus in Humans with COVID-19 Disease and Unexposed Individuals. Cell. 2020;181(7):1489-1501.e15.

12. Hartley GE, Edwards ESJ, Aui PM, Varese N, Stojanovic S, McMahon J, et al. Rapid generation of durable B cell memory to SARS-CoV-2 spike and nucleocapsid proteins in COVID-19 and convalescence. Sci Immunol. 2020;5(54):1–15.

13. Lucas C, Wong P, Klein J, Castro TBR, Silva J, Sundaram M, et al. Longitudinal analyses reveal immunological misfiring in severe COVID-19. Nature. 2020;584(7821):463–9.

14. Rodda LB, Netland J, Shehata L, Pruner KB, Morawski PA, Thouvenel CD, et al. Functional SARS-CoV-2-Specific Immune Memory Persists after Mild COVID-19. Cell. 2021.

15. Definitions C. WHO-2019-nCoV-Surveillance_Case_Definition-2020.2-eng. 2020;(December):2020.

16. Amanat F, Stadlbauer D, Strohmeier S, Nguyen THO, Chromikova V, McMahon M, et al. A serological assay to detect SARS-CoV-2 seroconversion in humans. Nat Med. 2020.

17. Stadlbauer D, Amanat F, Chromikova V, Jiang K, Strohmeier S, Arunkumar GA, et al. SARS-CoV-2 Seroconversion in Humans: A Detailed Protocol for a Serological Assay, Antigen Production, and Test Setup. Curr Protoc Microbiol. 2020;57(1):1–15.

18. Champagne P, Ogg GS, King AS, Knabenhans C, Ellefsen K, Nobile M, et al. Skewed maturation of memory HIV-specific CD8 T lymphocytes. Nature. 2001;410(6824):106–11.

19. Miller JD, van der Most RG, Akondy RS, Glidewell JT, Albott S, Masopust D, et al. Human Effector and Memory CD8+ T Cell Responses to Smallpox and Yellow Fever Vaccines. Immunity. 2008;28(5):710–22.

20. Weiskopf D, Bangs DJ, Sidney J, Kolla R V., De Silva AD, De Silva AM, et al. Dengue virus infection elicits highly polarized CX3CR1+ cytotoxic CD4+ T cells associated with protective immunity. Proc Natl Acad Sci U S A. 2015;112(31):E4256–63.

21. Huang AT, Garcia-Carreras B, Hitchings MDT, Yang B, Katzelnick L, Rattigan SM, et al. A systematic review of antibody mediated immunity to coronaviruses: antibody kinetics, correlates of protection, and association of antibody responses with severity of disease. medRxiv. 2020;2020.04.14.20065771.

22. Mathew D, Giles JR, Baxter AE, Oldridge DA, Greenplate AR, Wu JE, et al. Deep immune profiling of COVID-19 patients reveals distinct immunotypes with therapeutic implications. Science (80- ). 2020;369(6508).

23. Le Bert N, Tan AT, Kunasegaran K, Tham CYL, Hafezi M, Chia A, et al. SARS-CoV-2-specific T cell immunity in cases of COVID-19 and SARS, and uninfected controls. Nature. 2020;584(7821):457–62.

24. Dong Y, Dong Y, Mo X, Hu Y, Qi X, Jiang F, et al. Epidemiology of COVID-19 among children in China. Pediatrics. 2020;145(6).

25. Bunyavanich S, Do A, Vicencio A. Nasal Gene Expression of Angiotensin-Converting Enzyme 2 in Children and Adults. JAMA - Journal of the American Medical Association. 2020.

26. Hyde Z. COVID-19, children and schools: overlooked and at risk. Med J Aust. 2020.
27. Liu YJ. Dendritic cell subsets and lineages, and their functions in innate and adaptive immunity. Cell. 2001;106(3):259–62.
28. Zhou R, To KKW, Wong YC, Liu L, Zhou B, Li X, et al. Acute SARS-CoV-2 Infection Impairs Dendritic Cell and T Cell Responses. Immunity. 2020;53(4):864-877.e5.
29. Steinman RM. Decisions about dendritic cells: Past, present, and future. Annu Rev Immunol. 2012;30:1–22.
30. Boeddha NP, Kerklaan D, Dunbar A, van Puffelen E, Nagtzaam NMA, Vanhorebeek I, et al. HLA-DR Expression on Monocyte Subsets in Critically Ill Children. Pediatr Infect Dis J. 2018;37(10):1034–40.
31. Choi JY, Kim JH, Hossain FMA, Uyangaa E, Park SO, Kim B, et al. Indispensable role of CX3CR1+ dendritic cells in regulation of virus-induced neuroinflammation through rapid development of antiviral immunity in peripheral lymphoid tissues. Front Immunol. 2019;10(JUN):1–24.
32. Hamon P, Loyher PL, De Chanville CB, Licata F, Combadìere C, Boissonnas A. CX3CR1-dependent endothelial margination modulates Ly6Chigh monocyte systemic deployment upon inflammation in mice. Blood. 2017;129(10):1296–307.
33. Hu Y, Wen J, Tang L, Zhang H, Zhang X, Li Y, et al. The M protein of SARS-CoV: basic structural and immunological properties. Genomics, proteomics Bioinforma / Beijing Genomics Inst. 2003;1(2):118–30.
34. Thieme CJ, Anft M, Paniskaki K, Blazquez-Navarro A, Doevelaar A, Seibert FS, et al. Robust T Cell Response Toward Spike, Membrane, and Nucleocapsid SARS-CoV-2 Proteins Is Not Associated with Recovery in Critical COVID-19 Patients. Cell Reports Med. 2020;1(6):100092.

673 35. De Wit E, Van Doremalen N, Falzarano D, Munster VJ. SARS and MERS: Recent
674 insights into emerging coronaviruses. Nat Rev Microbiol. 2016;14(8):523–34.
675 36. Wu HS, Hsieh YC, Su IJ, Lin TH, Chiu SC, Hsu YF, et al. Early detection of
676 antibodies against various structural proteins of the SARS-associated coronavirus in
677 SARS patients. J Biomed Sci. 2004;11(1):117–26.
678 37. Ferretti AP, Kula T, Wang Y, Nguyen DMV, Weinheimer A, Dunlap GS, et al.
679 Unbiased Screens Show CD8+ T Cells of COVID-19 Patients Recognize Shared
680 Epitopes in SARS-CoV-2 that Largely Reside outside the Spike Protein. Immunity.
681 2020.
682 38. Cohen CA, Li AP, Hachim A, Hui DS, Kwan MY, Tsang OT, et al. SARS-CoV-2
683 specific T cell responses are lower in children and increase with age and time after
684 infection. medRxiv Prepr Serv Heal Sci. 2021.
685 39. Anderson EM, Goodwin EC, Verma A, Arevalo CP, Bolton MJ, Weirick ME, et al.
686 Seasonal human coronavirus antibodies are boosted upon SARS-CoV-2 infection but
687 not associated with protection. Cell. 2021;1858–64.
688 40. Alison Tarke A, Sidney J, Methot N, Zhang Y, Dan JM, Goodwin B, et al. Negligible
689 impact of SARS-CoV-2 variants on CD4 + and CD8 + T cell reactivity in COVID-19
690 exposed donors and vaccinees. bioRxiv. 2021;2021.02.27.433180.
691

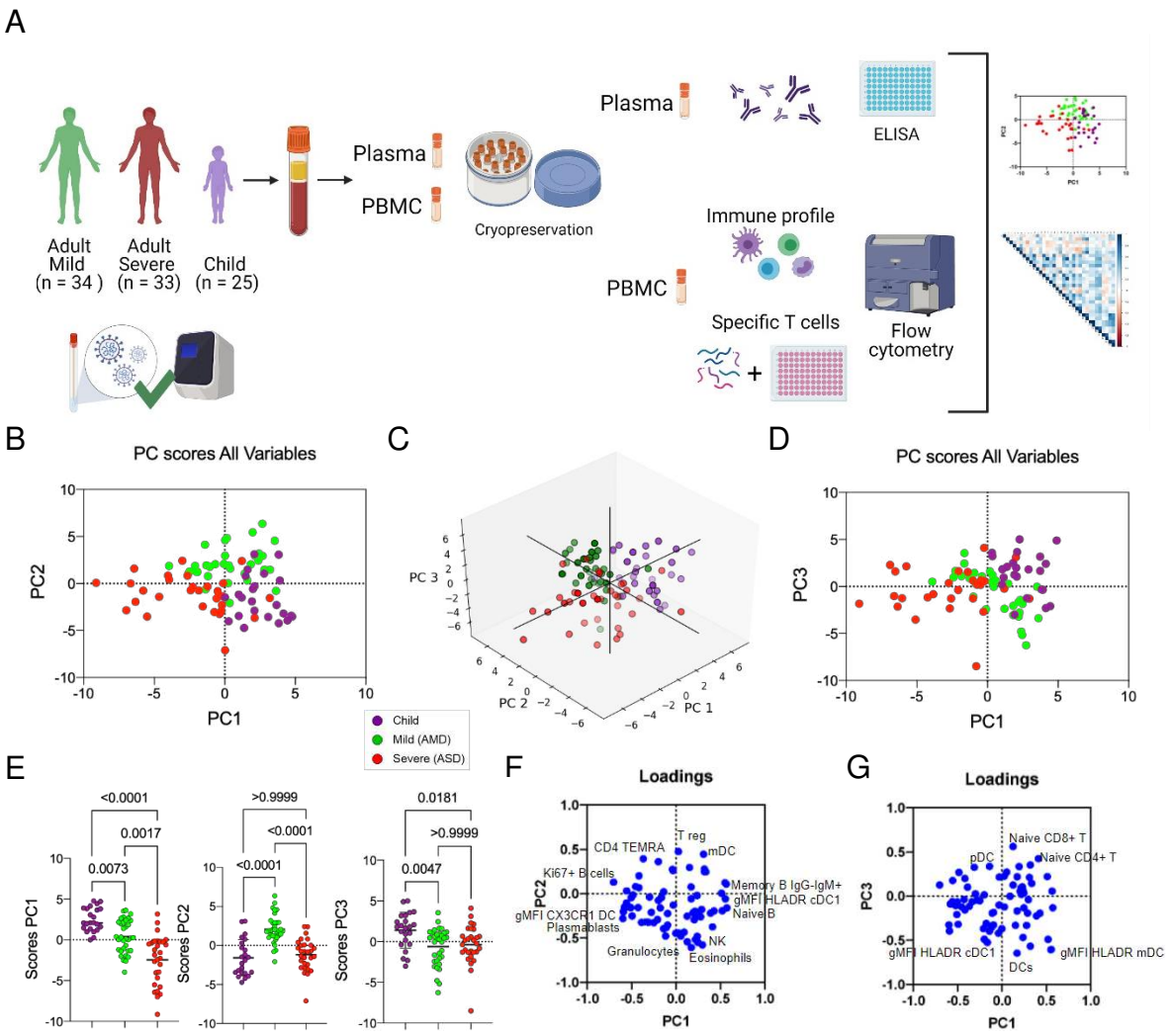


692

693 **Figure 1**: **Experimental approach and differential immune profile of children, mild and**
694 **adult patients by principal component analysis. A**, Graphical representation of the study
695 design; **B-E**, Principal component analysis of the clusters of pediatric (purple) and adult
696 patients with mild (green) and severe (red) disease; each dot represents a patient, color
697 coded. **B**, distribution of clusters by PC1 and PC2; **C**, 3D representation including PC1, 2
698 and 3; **D**, two-dimensional plot of patients according to PC3 by PC1; **E**, comparison of
699 scores for each PC by analysis of variance (Kruskal-Wallis). **F-G**, Contribution of variables
700 (loadings) to PC1xPC2 (**F**) and PC1xPC3 (**G**). Each blue dot is a variable. Variables with
701 the highest contributions (negative or positive) to each PC are specified. P values are
702 indicated over brackets.

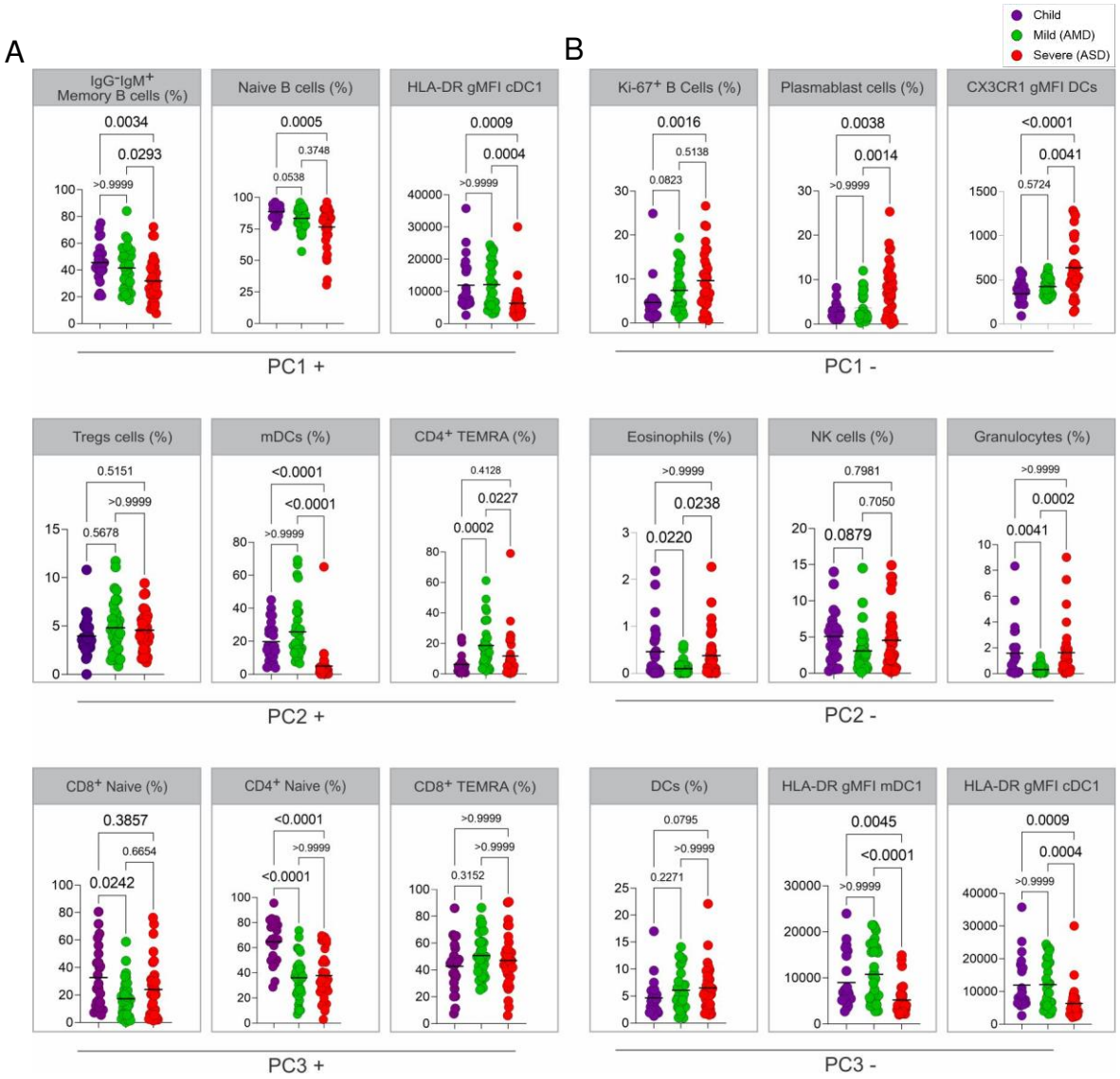


**Figure 2**. **Analysis of variance of the main variables contributing to principal components. A-B**, Kruskal-Wallis tests comparing values of each of the three immune variables that presented the highest influences – either positive (**A**) or negative (**B**) for PC1, PC2 and PC3. Each dot represents a patient, color coded: children – purple, adult with mild disease – green, and adult with severe disease – red. P values are indicated over brackets.

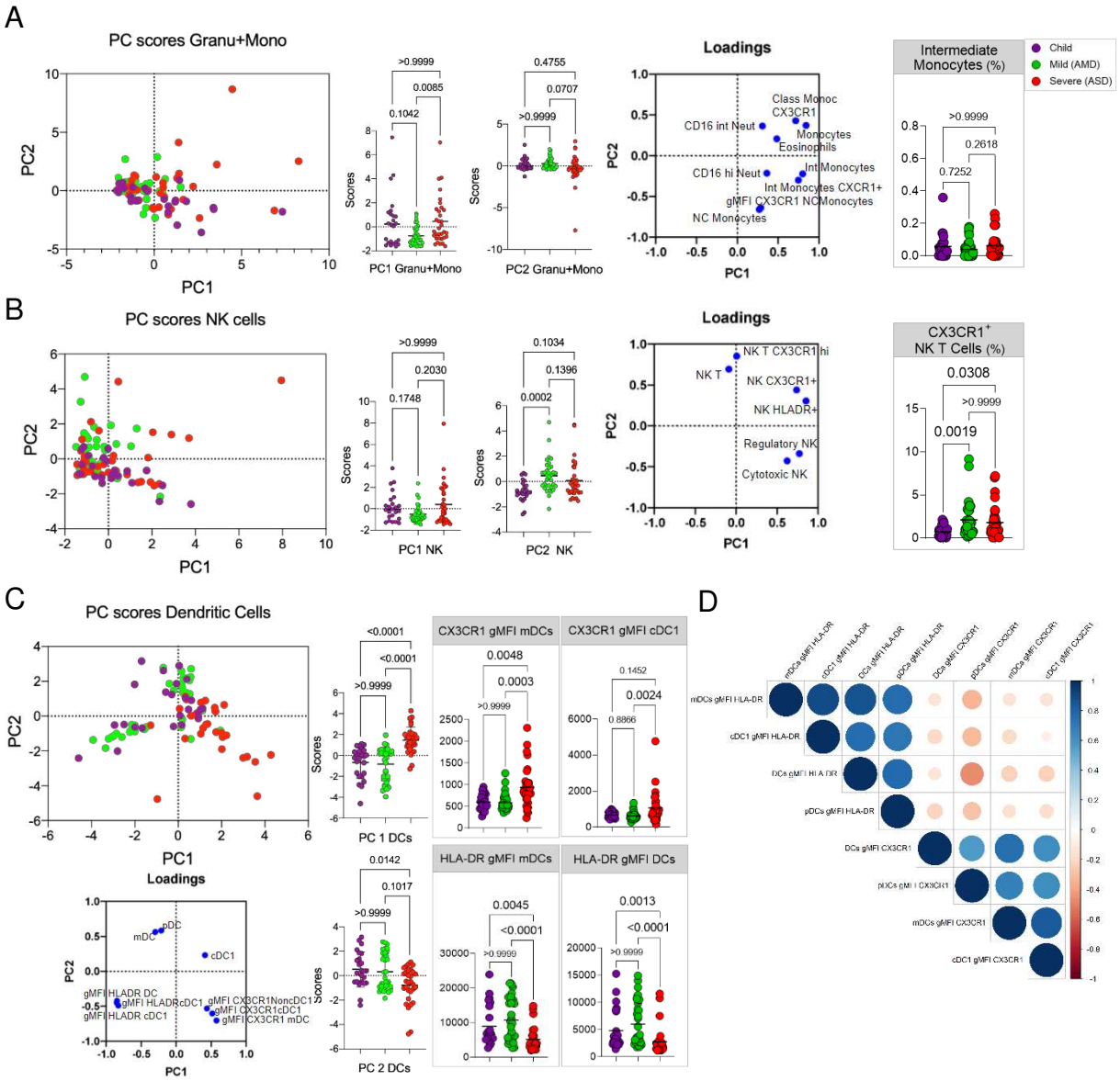


709

710 **Figure 3**. **Principal Component Analysis of innate cells immune signatures. A-G**,
711 Principal component analysis of the clusters of patients (each dot representing a patient,
712 color coded), according to the immune signatures (**A**, Granu$^{+}$Mono, Granulocytes and
713 Monocytes; **B**, NK cells; **C**, Dendritic Cells; **D**, Spearman correlation analysis of HLA-DR
714 and CX3CR1 expression in DCS. For each signature, are displayed the PCA plot of
715 PC1xPC2, the differences in scores of individuals for each PC; the loadings of the main
716 variables contributing to each PC and Kruskal-Wallis tests comparisons of the major
717 contributing variables values for each group of patients.

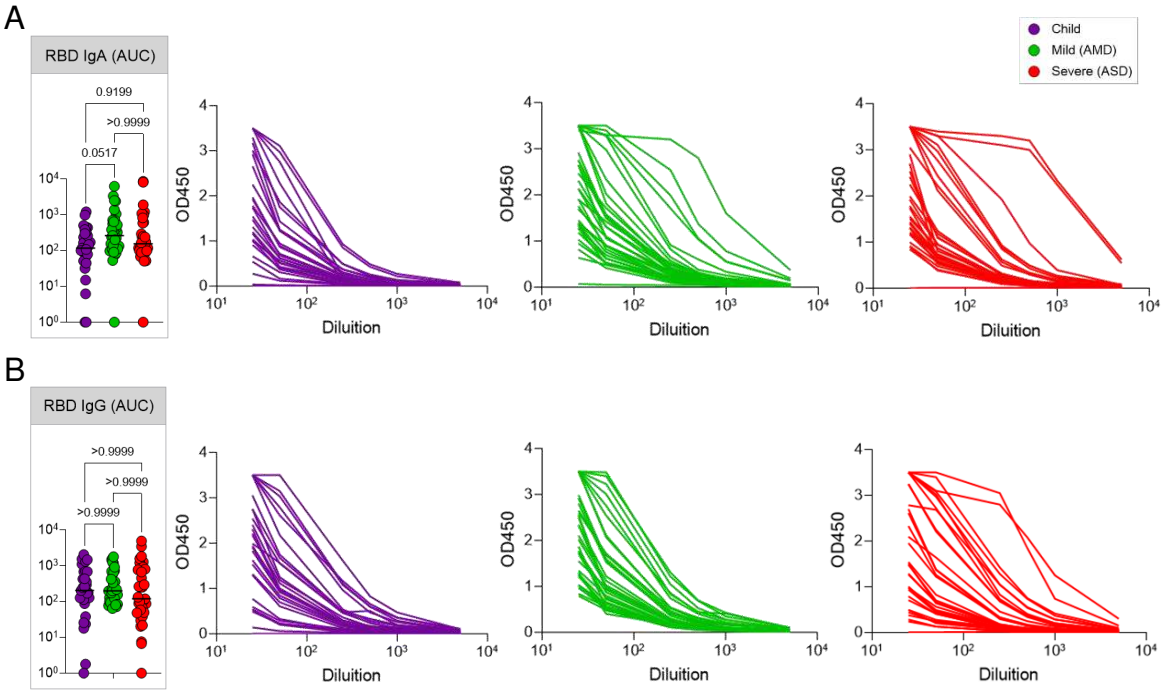


**Figure 4**. **Antibody responses.** SARS-CoV-2 spike RBD IgA and IgG antibody titers determined by ELISA using serial dilutions of plasma. Individual titration curves for each individual (represented by a line, color coded) and analysis of variance (Kruskal-Wallis) of the values calculated as the area under the curve (AUC) for IgA (**A**) and IgG (**B**) are displayed. P values are displayed over brackets.

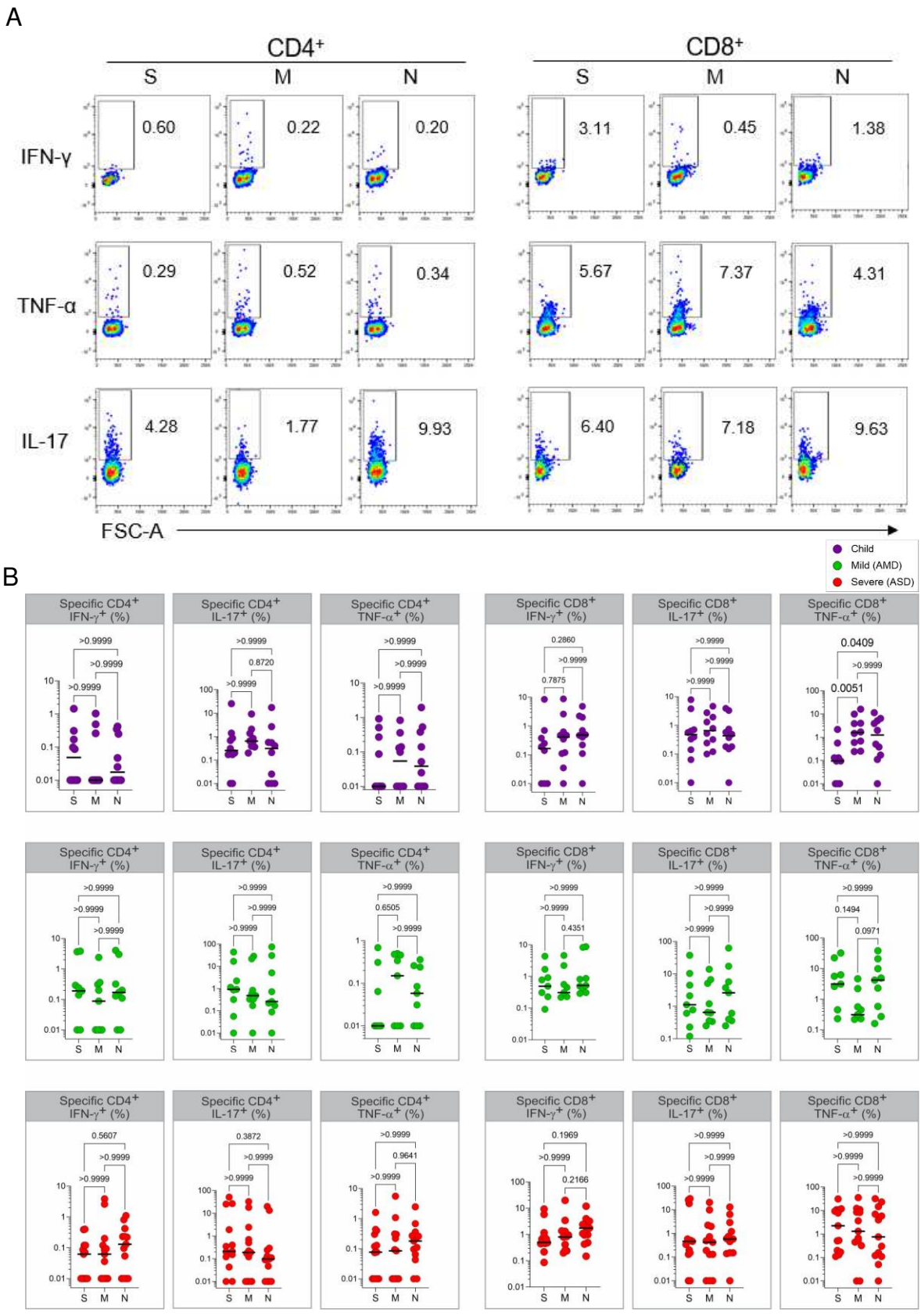
A
CD4+
CD8+
S
M
N
IFN-γ
TNF-α
IL-17
0.60
0.22
0.20
3.11
0.45
1.38
0.29
0.52
0.34
5.67
7.37
4.31
4.28
1.77
9.93
6.40
7.18
9.63
FSC-A
Child
Mild (AMD)
Severe (ASD)
B
Specific CD4+ IFN-γ+ (%)
Specific CD4+ IL-17+ (%)
Specific CD4+ TNF-α+ (%)
Specific CD8+ IFN-γ+ (%)
Specific CD8+ IL-17+ (%)
Specific CD8+ TNF-α+ (%)
>0.9999
0.8720
0.2860
0.7875
0.0409
0.0051
0.6505
0.4351
0.1494
0.0971
0.5607
0.3872
0.9641
0.1969
0.2166

724

725

726 **Figure 5**. **Specific T cell responses**. **A**, gating strategies and typical plots of CD4+ and
727 CD8+ T cells stimulated with peptide pools from structural proteins spike (S), membrane
728 (M) and nucleocapsid (N), and analyzed by flow cytometry for cytokine production. **B**,
729 Comparisons of effector T cells in each group - percentages of CD4+ or CD8+ cells,
730 producing INFγ, TNFα or IL-17 in response to stimulation by each peptide pool. Each dot
731 represents a patient, color coded: purple for children; green for adults with mild disease and
732 red for adults with severe disease. All analyses are Kruskal-Wallis tests, and the p values are
733 indicated over brackets. Significant differences are indicated by p values in a higher font.

A

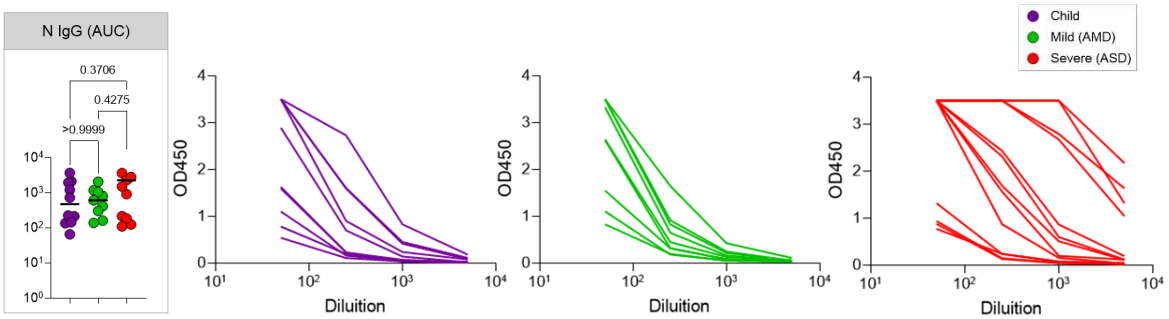
N IgG (AUC)
0.3706
0.4275
>0.9999
Child
Mild (AMD)
Severe (ASD)
OD450
Dilution

B

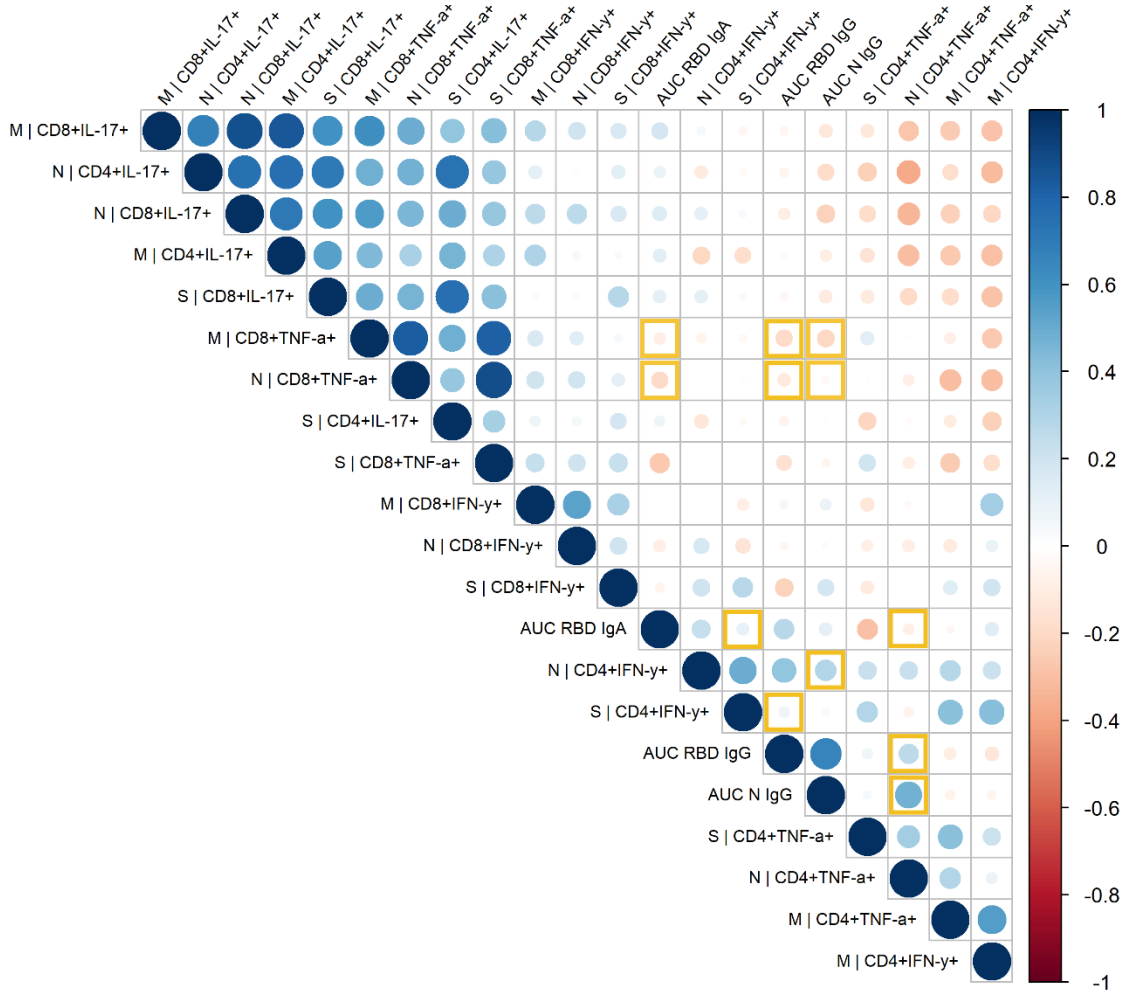
M | CD8+IL-17+
N | CD4+IL-17+
N | CD8+IL-17+
M | CD4+IL-17+
S | CD8+IL-17+
M | CD8+TNF-a+
N | CD8+TNF-a+
S | CD4+IL-17+
S | CD8+TNF-a+
M | CD8+IFN-y+
N | CD8+IFN-y+
S | CD8+IFN-y+
AUC RBD IgA
N | CD4+IFN-y+
S | CD4+IFN-y+
AUC RBD IgG
AUC N IgG
S | CD4+TNF-a+
N | CD4+TNF-a+
M | CD4+TNF-a+
M | CD4+IFN-y+
1
0.8
0.6
0.4
0.2
0
-0.2
-0.4
-0.6
-0.8
-1

734

735

736 **Figure 6**. **Anti-N IgG response and correlation of specific responses. A**, SARS-CoV-2
737 anti-N IgG antibody titers determined by ELISA using serial dilutions of plasma. Individual
738 titration curves for each individual (represented by a line, color coded) and analysis of
739 variance (Kruskal-Wallis) of the values calculated as the area under the curve (AUC) for
740 IgG (**A**) are displayed. P values are displayed over brackets. **B**, Matrix representing a
741 Spearman correlation analysis of specific effector T cells responses (in percentages of
742 positive CD4+ and CD8+ positive cytokine expressing cells in response to peptide pools)
743 and the antibody response to the RBD of the spike protein and to the N protein (represented
744 as values for the AUC). Correlations between the specific effector CD8+ T and CD4+ T
745 cells frequencies, and the antibody (AUC – area under the curve) values for the RBD and N
746 protein are highlighted.

747

**Table 1.** Clinical characteristics of all patients in this study.

| **Characteristics** | **Mild (n = 34)** | **Severe (n = 33)** | **Children (n = 25)** | **P-value** |
|---|---|---|---|---|
| Age (y), median (IQR) | 37.8 (27.0-44.6) | 60.8 (38.8-75.9) | 9.0 (1.5-13.5) | **<0.0001*** |
| Female sex, n (%) | 22 (64.7) | 17 (51.5) | 10 (42.0) | 0.1657† |
| Active or passive smoking, n (%) | 2 (5.9) | 6 (18.2) | 3 (12.0) | 0.0791† |
| **Racial or ethnic group** | | | | |
| Caucasian, n (%) | 28 (82.4) | 20 (60.6) | 17 (68.0) | 0.1129† |
| Non-caucasian, n (%) | 4 (11.8) | 1 (3.0) | 5 (20.0) | |
| **Days from of symptom onset to sample collection** | | | | |
| Days, median (IQR) | 18.0 (16.0-20.5) | 10.0 (7.5-14.0) | 15.0 (8.5-17.5) | **<0.0001**** |
| **Symptoms** | | | | |
| Headache, n (%) | 32 (94.1) | 23 (69.7) | 14 (56.0) | **0.0262†** |
| Myalgia, n (%) | 30 (88.2) | 20 (60.6) | 9 (36.0) | **0.0030†** |
| Malaise, n (%) | 28 (82.4) | 31 (93.9) | 14 (56.0) | **0.0006†** |
| Coryza, n (%) | 26 (76.5) | 18 (54.5) | 16 (64.0) | 0.2167† |
| Cough, n (%) | 25 (73.5) | 30 (90.9) | 17 (68.0) | 0.0782† |
| Fever, n (%) | 23 (67.6) | 26 (78.8) | 20 (80.0) | 0.4899† |
| Chills, n (%) | 21 (61.8) | 20 (60.6) | 9 (36.0) | 0.0823† |
| Dyspnea, n (%) | 20 (58.8) | 22 (66.7) | 4 (16.0) | **0.0003†** |
| Dysgeusia, n (%) | 20 (58.8) | 12 (36.4) | 6 (24.0) | 0.1580† |
| Sore throat, n (%) | 19 (55.9) | 12 (36.4) | 11 (44.0) | 0.2986† |
| Appetite loss, n (%) | 19 (55.9) | 21 (63.6) | 13 (52.0) | 0.6226† |
| Anosmia, n (%) | 19 (55.9) | 11 (33.3) | 6 (24.0) | 0.1841† |
| Stuffy nose, n (%) | 17 (50.0) | 11 (33.3) | 13 (52.0) | 0.3868† |
| Conjuctivitis, n (%) | 16 (47.1) | 10 (30.3) | 7 (28.0) | 0.2465† |
| Nausea, n (%) | 14 (41.2) | 12 (36.4) | 7 (28.0) | 0.7791† |

| | | | | |
|---|---|---|---|---|
| Sputum production, n (%) | 12 (35.3) | 10 (30.3) | 6 (24.0) | 0.6420† |
| Diarrhea, n (%) | 12 (35.3) | 16 (48.5) | 7 (28.0) | 0.2122† |
| Vomiting, n (%) | 2 (5.9) | 4 (12.1) | 4 (16.0) | 0.4442† |
| Skin rash, n (%) | 1 (2.9) | 1 (3.0) | 1 (4.0) | 0.9744† |
| **Underlying medical conditions** | | | | |
| Obesity, n (%) | 10 (29.4) | 13 (39.4) | 0 (0.0) | **0.0021†** |
| Hypertension, n (%) | 6 (17.6) | 15 (45.5) | 0 (0.0) | **0.0111†** |
| Asthma, n (%) | 1 (2.9) | 2 (6.1) | 6 (24.0) | **<0.0001†** |
| Diabetes mellitus, type 1 and 2, n (%) | 1 (2.9) | 11 (33.3) | 0 (0.0) | **0.0362†** |
| Cancer, n (%) | 1 (2.9) | 2 (6.1) | 0 (0.0) | 0.7180† |
| Tuberculosis, n (%) | 0 (0.0) | 1 (3.0) | 0 (0.0) | 0.7809† |
| Stroke/CVA, n (%) | 0 (0.0) | 4 (12.1) | 0 (0.0) | 0.2168† |
| COPD, n (%) | 0 (0.0) | 4 (12.1) | 1 (4.2) | 0.4088† |
| Heart failure, n (%) | 0 (0.0) | 2 (6.1) | 0 (0.0) | 0.6926† |
| Congenital heart disease, n (%) | 0 (0.0) | 1 (3.0) | 0 (0.0) | 0.7044† |
| **Ct value (median, IQR)** | | | | |
| ORF1ab | 19.3 (16.7-22.6) | 24.3 (19.9-29.7) | 19.8 (15.4-27.5) | **0.0488**** |
| S | 19.8 (16.7-23.0) | 25.3 (21.9-27.7) | 19.4 (13.2-28.3) | **0.0239**** |
| N | 18.7 (16.1-23.5) | 24.0 (20.6-28.6) | 19.7 (14.1-29.2) | **0.0201**** |
| **Oxigen use** | | | | |
| Oxigen use during hospitalization, n (%) | 0 (0.0) | 22 (66.7) | 0 (0.0) | **<0.0001†** |

IQR = interquartile range; ** Kruskal-Wallis test; † Pearson's Chi-squared test

748

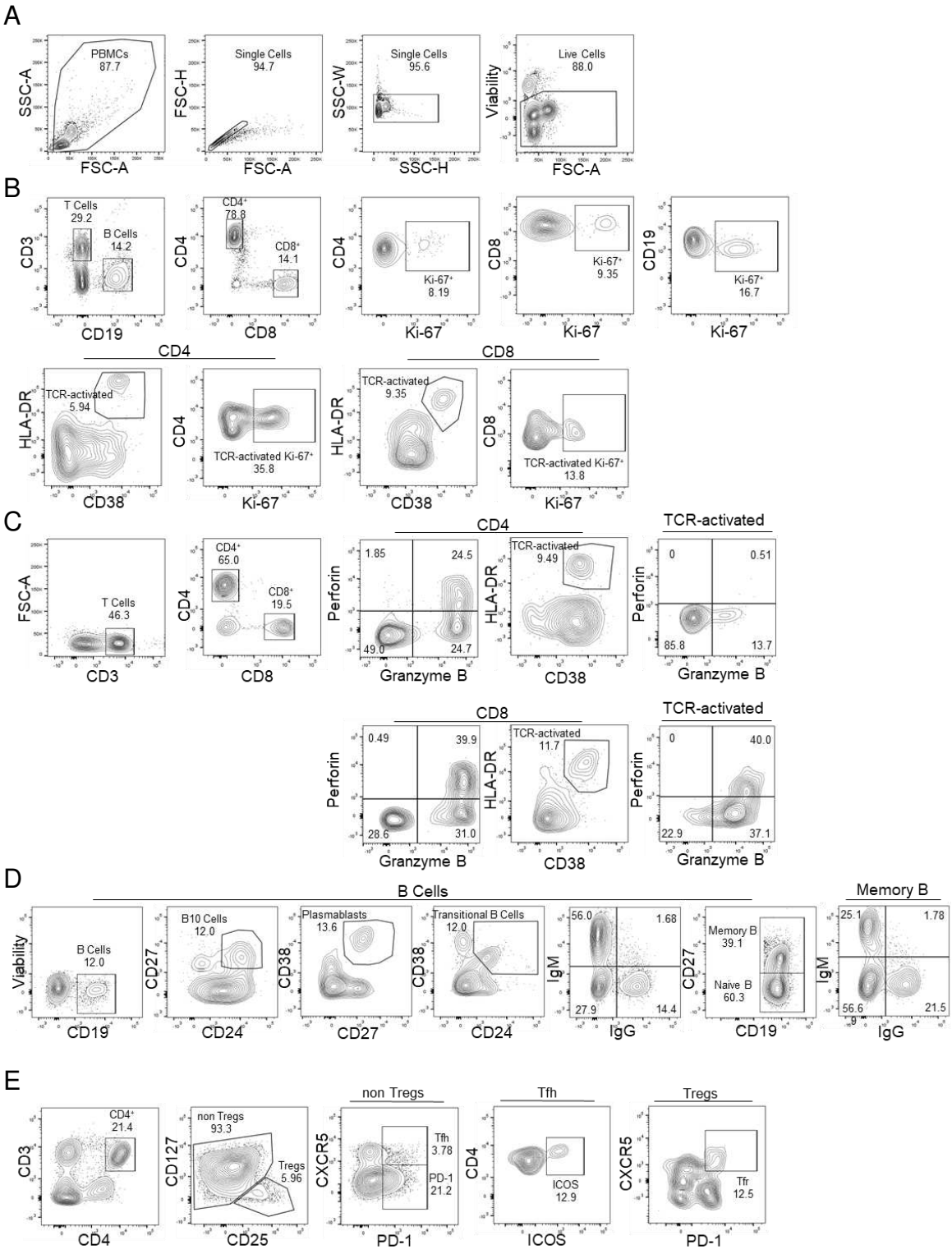
A
PBMCs
87.7
SSC-A
FSC-A
Single Cells
94.7
FSC-H
FSC-A
Single Cells
95.6
SSC-W
SSC-H
Live Cells
88.0
Viability
FSC-A
B
T Cells
29.2
B Cells
14.2
CD3
CD19
CD4+
78.8
CD8+
14.1
CD4
CD8
Ki-67+
8.19
CD4
Ki-67
Ki-67+
9.35
CD8
Ki-67
Ki-67+
16.7
CD19
Ki-67
CD4
CD8
TCR-activated
5.94
HLA-DR
CD38
TCR-activated Ki-67+
35.8
CD4
Ki-67
TCR-activated
9.35
HLA-DR
CD38
TCR-activated Ki-67+
13.8
CD8
Ki-67
C
T Cells
46.3
FSC-A
CD3
CD4+
65.0
CD8+
19.5
CD4
CD8
CD4
1.85
24.5
49.0
24.7
Perforin
Granzyme B
TCR-activated
9.49
HLA-DR
CD38
TCR-activated
0
0.51
85.8
13.7
Perforin
Granzyme B
CD8
0.49
39.9
28.6
31.0
Perforin
Granzyme B
TCR-activated
11.7
HLA-DR
CD38
TCR-activated
0
40.0
22.9
37.1
Perforin
Granzyme B
D
B Cells
Memory B
Viability
B Cells
12.0
CD19
CD27
B10 Cells
12.0
CD24
CD38
Plasmablasts
13.6
CD27
CD38
Transitional B Cells
12.0
CD24
IgM
56.0
1.68
27.9
14.4
IgG
CD27
Memory B
39.1
Naive B
60.3
CD19
IgM
25.1
1.78
56.6
21.5
IgG
E
CD4+
21.4
CD3
CD4
non Tregs
93.3
Tregs
5.96
CD127
CD25
non Tregs
Tfh
3.78
PD-1
21.2
CXCR5
PD-1
Tfh
ICOS
12.9
CD4
ICOS
Tregs
Tfr
12.5
CXCR5
PD-1

749

F

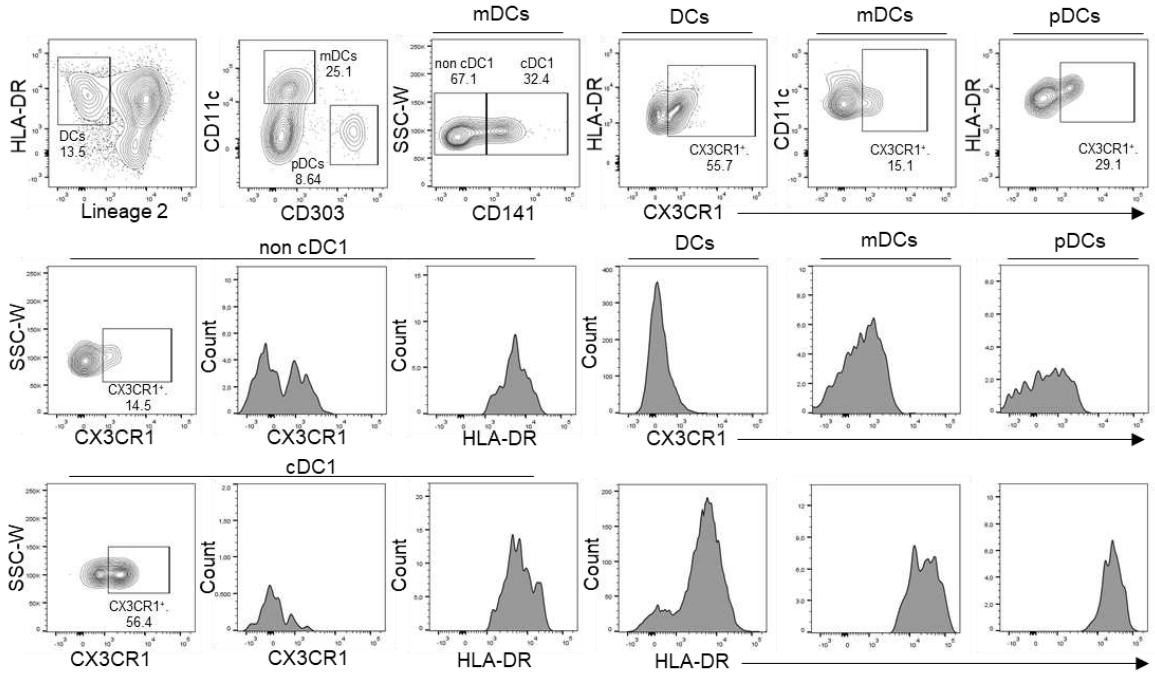
mDCs
DCs
mDCs
pDCs
HLA-DR
DCs
13.5
Lineage 2
CD11c
mDCs
25.1
pDCs
8.64
CD303
SSC-W
non cDC1
67.1
cDC1
32.4
CD141
HLA-DR
CX3CR1+
55.7
CX3CR1
CD11c
CX3CR1+
15.1
HLA-DR
CX3CR1+
29.1
non cDC1
DCs
mDCs
pDCs
SSC-W
CX3CR1+
14.5
CX3CR1
Count
CX3CR1
Count
HLA-DR
Count
CX3CR1
Count
cDC1
SSC-W
CX3CR1+
56.4
CX3CR1
Count
CX3CR1
Count
HLA-DR
Count
HLA-DR

G

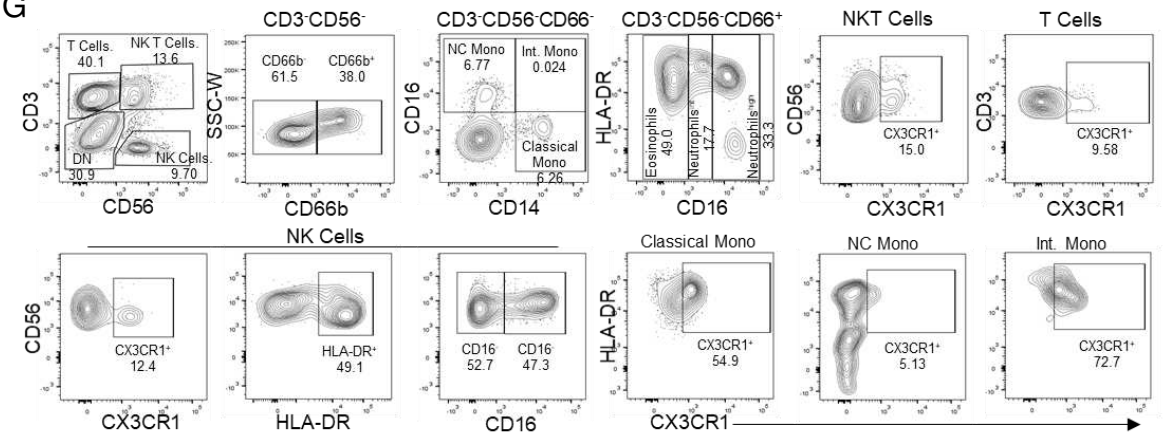
CD3-CD56-
CD3-CD56-CD66-
CD3-CD56-CD66+
NKT Cells
T Cells
T Cells.
40.1
NK T Cells.
13.6
CD3
DN
30.9
NK Cells.
9.70
CD56
SSC-W
CD66b-
61.5
CD66b+
38.0
CD66b
CD16
NC Mono
6.77
Int. Mono
0.024
Classical
Mono
6.26
CD14
HLA-DR
Eosinophils
49.0
Neutrophils+
17.7
Neutrophils++
33.3
CD16
CD56
CX3CR1+
15.0
CX3CR1
CD3
CX3CR1+
9.58
CX3CR1
NK Cells
Classical Mono
NC Mono
Int. Mono
CD56
CX3CR1+
12.4
CX3CR1
HLA-DR+
49.1
HLA-DR
CD16-
52.7
CD16-
47.3
CD16
HLA-DR
CX3CR1+
54.9
CX3CR1
CX3CR1+
5.13
CX3CR1+
72.7

H

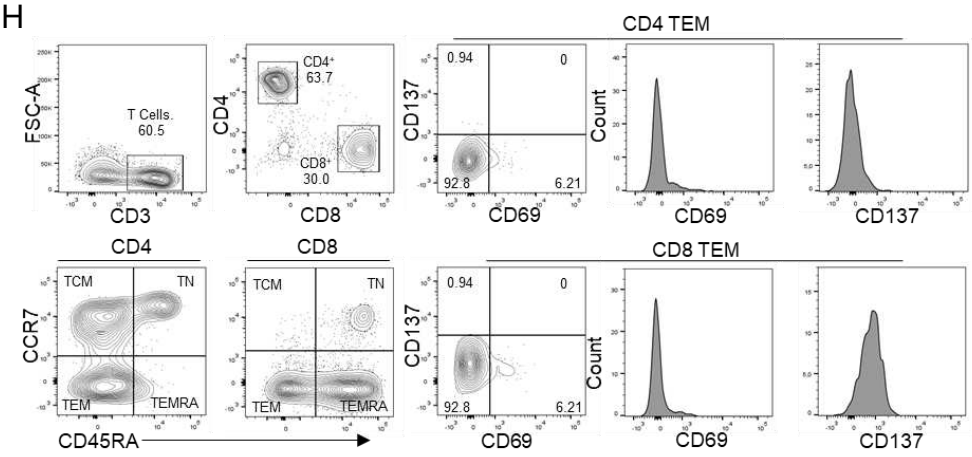
CD4 TEM
FSC-A
T Cells.
60.5
CD3
CD4
CD4+
63.7
CD8+
30.0
CD8
CD137
0.94
0
92.8
6.21
CD69
Count
CD69
CD137
CD4
CD8
CD8 TEM
CCR7
TCM
TN
TEM
TEMRA
CD45RA
TCM
TN
TEM
TEMRA
CD137
0.94
0
92.8
6.21
CD69
Count
CD69
CD137

750

**Supplementary Figure 1. Gating strategies for the key cell populations described in Fig. 1-4, Fig. 6A-B, Fig. 7, and other supplementary figures. A**, Gating strategy to identify all populations described in B-H. **B**, B and T cell surface staining gating strategy to identify B cells proliferation, CD4 and CD8 T cells, proliferation and TCR-activated T cells. **C**, T cell surface staining gating strategy to identify CD4 and CD8 T cells producing granzyme B and perforin in the population with or without TCR-activated T cells. **D**, B cell surface staining gating strategy to identify B10 cells, plasmablasts, transitional B cells, IgM cells, IgG cells, memory and naive cells populations. **E**, T cell surface staining gating strategy to identify Treg and TFH CD4 cells population. **F**, DCs surface staining gating strategy to identify differences in HLA-DR and CX3CR1 expression in DCs, mDC and pDCs cell populations. **G**, Innate cells and T surface staining gating strategy to identify NK cells, NK T cells, Eosinophils, Neutrophils and Monocytes populations. **H**, T cell surface staining gating strategy to identify differences in CD137 and CD69 expression in CD4 and CD8 T cells effector memory, central memory, terminally differentiated and naive population.

767

A


768

B

| | | | | | |
|---|---|---|---|---|---|
| 1 | PBMCs | 27 | Naive B Cells | 53 | HLA-DR$^+$ NK Cells |
| 2 | T cells | 28 | PD-1$^+$ CD4$^+$ T | 54 | CX3CR1$^+$ NK T cells |
| 3 | CD4$^+$ | 29 | Tfh cells | 55 | CD66$^+$ Granulocytes |
| 4 | Ki-67$^+$ CD4$^+$ | 30 | ICOS$^+$ Tfh cells | 56 | CD66b$^+$ CD16 hi Neutrophils |
| 5 | TCR-activated CD4$^+$ | 31 | Treg | 57 | CD66b$^+$ CD16 int Neutrophils |
| 6 | TCR-activated Ki-67$^+$ CD4$^+$ | 32 | CXCR5$^+$ Treg | 58 | CD66b$^+$ CD16 low Eosinophils |
| 7 | CD8$^+$ | 33 | DCs | 59 | Classical Monocytes |
| 8 | Ki-67$^+$ CD8$^+$ | 34 | CX3CR1 gMFI DCs | 60 | Intermediate Monocytes |
| 9 | TCR-activated CD8$^+$ | 35 | HLA-DR gMFI DCs | 61 | NC Monocytes |
| 10 | TCR-activated Ki-67$^+$ CD8$^+$ | 36 | mDCs | 62 | CX3CR1$^+$ Classical Monocytes |
| 11 | GranzB$^+$Perf$^+$ CD4$^+$ | 37 | CX3CR1 gMFI mDCs | 63 | CX3CR1$^+$ Intermediate Monocytes |
| 12 | TCR-activated GranzB$^+$Perf$^+$ CD4$^+$ | 38 | HLA-DR gMFI mDCs | 64 | CX3CR1$^+$ NC Monocytes |
| 13 | GranzB$^+$Perf$^+$ CD8$^+$ | 39 | cDC1 | 65 | CX3CR1$^+$ T cells |
| 14 | TCR-activated GranzB$^+$Perf$^+$ CD8$^+$ | 40 | CX3CR1 gMFI cDC1 | 66 | CD4$^+$ TCM |
| 15 | B cells | 41 | HLA-DR gMFI cDC1 | 67 | CD4$^+$ T Naive |
| 16 | Ki-67$^+$ B cells | 42 | Non cDC1 | 68 | CD4$^+$ TEMRA |
| 17 | B10 cells | 43 | CX3CR1 gMFI Non cDC1 | 69 | CD4$^+$ TEM |
| 18 | Plasmoblasts | 44 | HLA-DR gMFI Non cDC1 | 70 | CD69$^+$ gMFI CD4$^+$ TEM |
| 19 | IgG$^-$IgM$^+$ B cells | 45 | pDCs | 71 | CD137$^+$ gMFI CD4$^+$ TEM |
| 20 | IgG$^+$IgM$^+$ B cells | 46 | CX3CR1 gMFI pDCs | 72 | CD8$^+$ |
| 21 | IgG$^+$IgM- B cells | 47 | HLA-DR gMFI pDCs | 73 | CD8$^+$ TCM |
| 22 | Transitional B cells | 48 | NK cells | 74 | CD8$^+$ T Naive |
| 23 | Memory B cells | 49 | CD16$^+$NK cells | 75 | CD8$^+$ TEMRA |
| 24 | IgG$^-$IgM$^+$ Memory B cells | 50 | CD16$^-$ NK cells | 76 | CD8$^+$ TEM |
| 25 | IgG$^+$IgM$^+$ Memory B cells | 51 | NK T cells | 77 | CD69$^+$ gMFI CD8$^+$ TEM |
| 26 | IgG$^+$IgM$^-$ Memory B cells | 52 | CX3CR1$^+$ NK Cells | 78 | CD137$^+$ gMFI CD8$^+$ TEM |

769

**Supplementary Figure 2**. **Spearman correlation of all variables composing the immune profile**. **A**, Clusters of more correlated variables are outlined and identified in a Spearman correlation matrix of all variables. **B**, List of immune variables indicated by numbers by which they are plotted on the matrix.

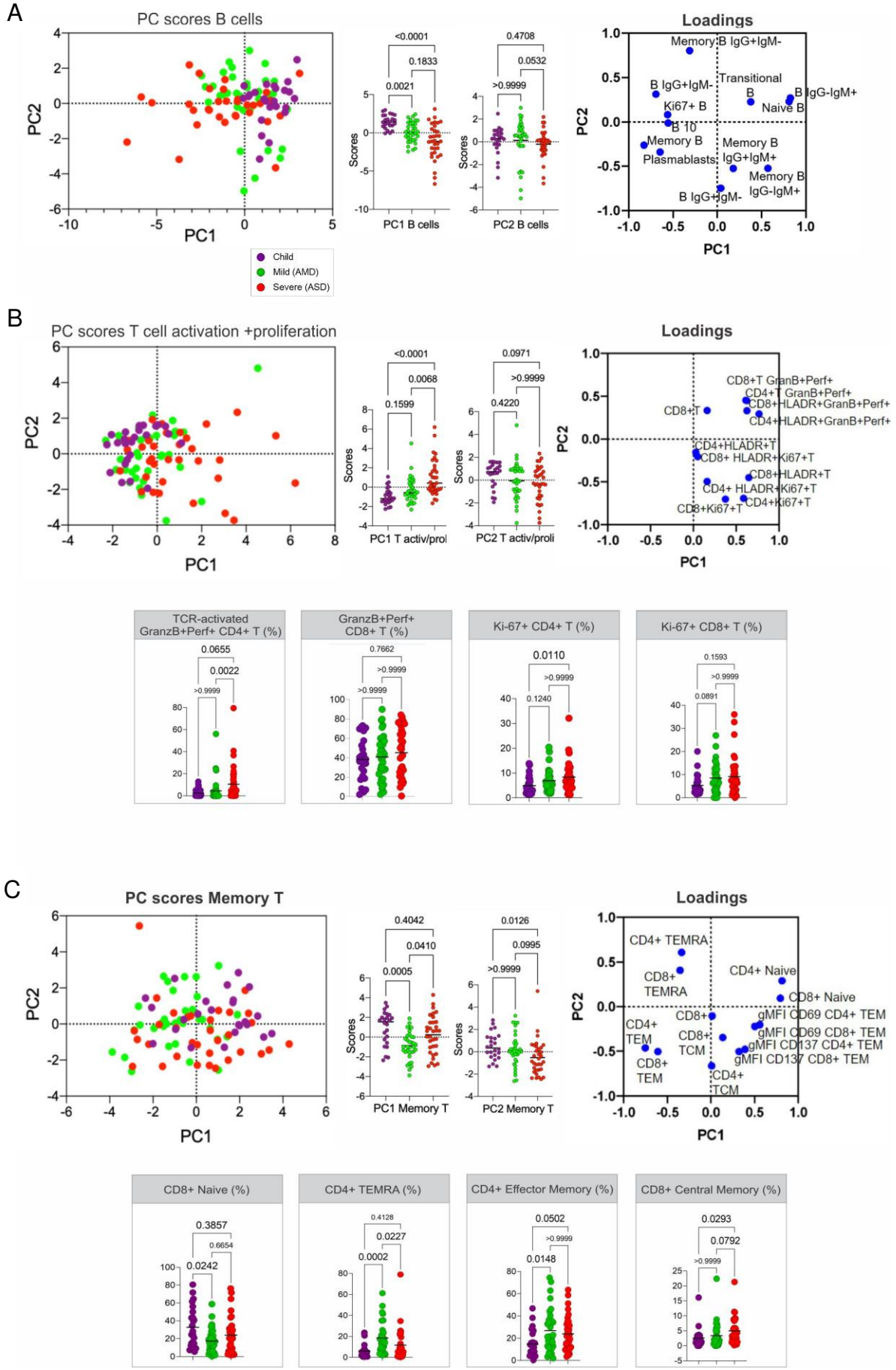
A
PC scores B cells
PC1
PC2
Child
Mild (AMD)
Severe (ASD)
<0.0001
0.1833
0.0021
PC1 B cells
0.4708
0.0532
>0.9999
PC2 B cells
Scores
Loadings
Memory B IgG+IgM-
B IgG+IgM-
Transitional B
B IgG-IgM+
Naive B
Ki67+ B
B 10
Memory B
Plasmablasts
Memory B IgG+IgM+
Memory B IgG-IgM+
B IgG+IgM-
B
PC scores T cell activation +proliferation
<0.0001
0.0068
0.1599
PC1 T activ/prol
0.0971
>0.9999
0.4220
PC2 T activ/proli
CD8+T GranB+Perf+
CD4+T GranB+Perf+
CD8+HLADR+GranB+Perf+
CD4+HLADR+GranB+Perf+
CD8+T
CD4+HLADR+T
CD8+ HLADR+Ki67+T
CD8+HLADR+T
CD4+ HLADR+Ki67+T
CD8+Ki67+T
CD4+Ki67+T
TCR-activated GranzB+Perf+ CD4+ T (%)
0.0655
0.0022
>0.9999
GranzB+Perf+ CD8+ T (%)
0.7662
>0.9999
>0.9999
Ki-67+ CD4+ T (%)
0.0110
>0.9999
0.1240
Ki-67+ CD8+ T (%)
0.1593
>0.9999
0.0891
C
PC scores Memory T
0.4042
0.0410
0.0005
PC1 Memory T
0.0126
0.0995
>0.9999
PC2 Memory T
CD4+ TEMRA
CD8+ TEMRA
CD4+ Naive
CD8+ Naive
CD8+
gMFI CD69 CD4+ TEM
CD4+ TEM
CD8+ TCM
gMFI CD69 CD8+ TEM
gMFI CD137 CD4+ TEM
gMFI CD137 CD8+ TEM
CD8+ TEM
CD4+ TCM
CD8+ Naive (%)
0.3857
0.6654
0.0242
CD4+ TEMRA (%)
0.4128
0.0227
0.0002
CD4+ Effector Memory (%)
0.0502
>0.9999
0.0148
CD8+ Central Memory (%)
0.0293
0.0792
>0.9999

**Supplementary Figure 3. Principal Component Analysis of adaptive cells immune signatures. A**, B cells; **B**, Proliferating/activated T cells; and **C**, Memory T cells). For each signature, are displayed the PCA plot of PC1xPC2, the differences in scores of individuals for each PC; the loadings of the main variables contributing to each PC; and Kruskal-Wallis tests comparisons of the major contributing variables values for each group of patients.

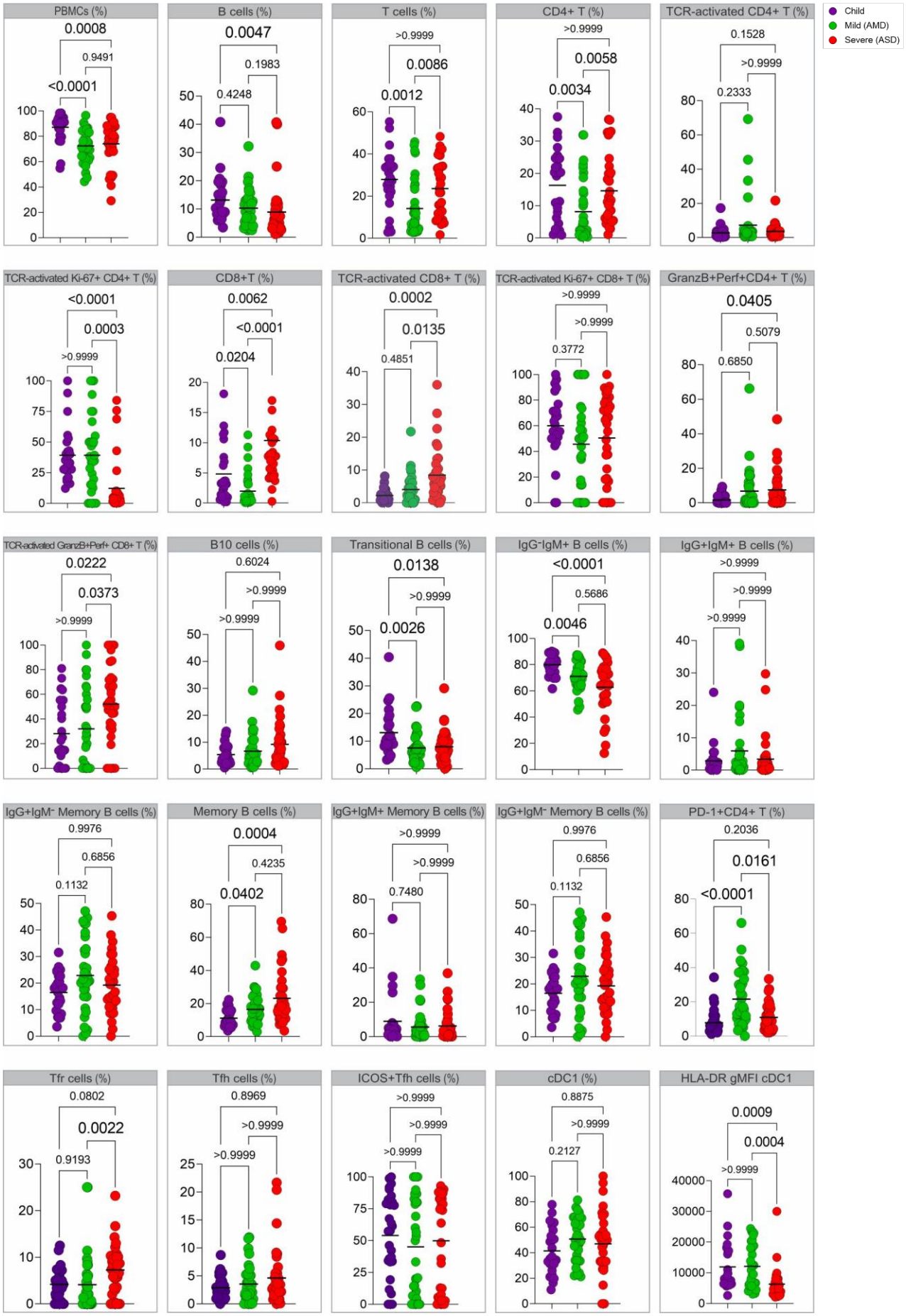
Child
Mild (AMD)
Severe (ASD)
PBMCs (%)
0.0008
0.9491
<0.0001
B cells (%)
0.0047
0.1983
0.4248
T cells (%)
>0.9999
0.0086
0.0012
CD4+ T (%)
>0.9999
0.0058
0.0034
TCR-activated CD4+ T (%)
0.1528
>0.9999
0.2333
TCR-activated Ki-67+ CD4+ T (%)
<0.0001
0.0003
>0.9999
CD8+T (%)
0.0062
<0.0001
0.0204
TCR-activated CD8+ T (%)
0.0002
0.0135
0.4851
TCR-activated Ki-67+ CD8+ T (%)
>0.9999
>0.9999
0.3772
GranzB+Perf+CD4+ T (%)
0.0405
0.5079
0.6850
TCR-activated GranzB+Perf+ CD8+ T (%)
0.0222
0.0373
>0.9999
B10 cells (%)
0.6024
>0.9999
>0.9999
Transitional B cells (%)
0.0138
>0.9999
0.0026
IgG-IgM+ B cells (%)
<0.0001
0.5686
0.0046
IgG+IgM+ B cells (%)
>0.9999
>0.9999
>0.9999
IgG+IgM- Memory B cells (%)
0.9976
0.6856
0.1132
Memory B cells (%)
0.0004
0.4235
0.0402
IgG+IgM+ Memory B cells (%)
>0.9999
>0.9999
0.7480
IgG+IgM- Memory B cells (%)
0.9976
0.6856
0.1132
PD-1+CD4+ T (%)
0.2036
0.0161
<0.0001
Tfr cells (%)
0.0802
0.0022
0.9193
Tfh cells (%)
0.8969
>0.9999
>0.9999
ICOS+Tfh cells (%)
>0.9999
>0.9999
>0.9999
cDC1 (%)
0.8875
>0.9999
0.2127
HLA-DR gMFI cDC1
0.0009
0.0004
>0.9999

782

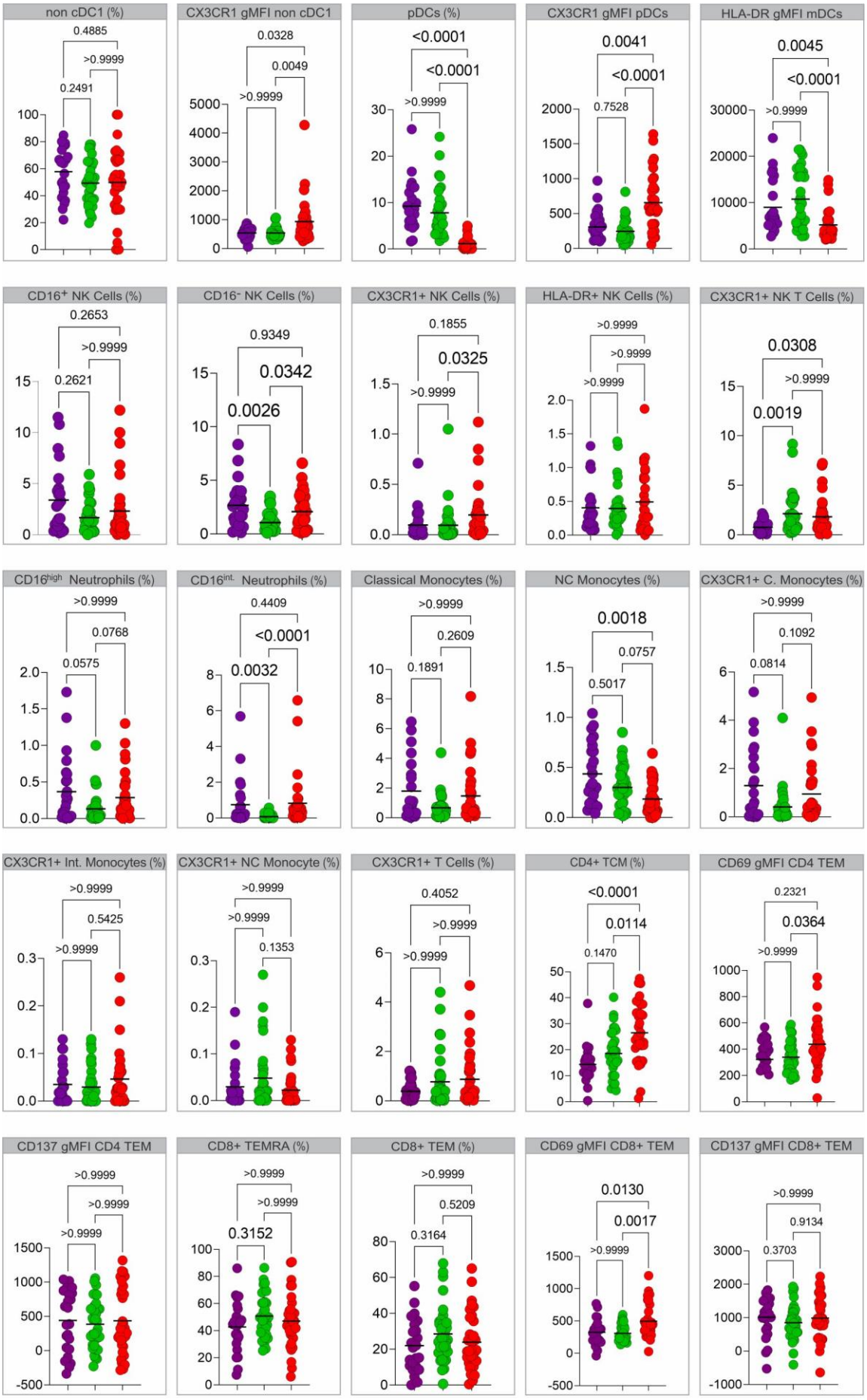
non cDC1 (%)
0.4885
>0.9999
0.2491
CX3CR1 gMFI non cDC1
0.0328
0.0049
>0.9999
pDCs (%)
<0.0001
<0.0001
>0.9999
CX3CR1 gMFI pDCs
0.0041
<0.0001
0.7528
HLA-DR gMFI mDCs
0.0045
<0.0001
>0.9999
CD16+ NK Cells (%)
0.2653
>0.9999
0.2621
CD16- NK Cells (%)
0.9349
0.0342
0.0026
CX3CR1+ NK Cells (%)
0.1855
0.0325
>0.9999
HLA-DR+ NK Cells (%)
>0.9999
>0.9999
>0.9999
CX3CR1+ NK T Cells (%)
0.0308
>0.9999
0.0019
CD16high Neutrophils (%)
>0.9999
0.0768
0.0575
CD16int. Neutrophils (%)
0.4409
<0.0001
0.0032
Classical Monocytes (%)
>0.9999
0.2609
0.1891
NC Monocytes (%)
0.0018
0.0757
0.5017
CX3CR1+ C. Monocytes (%)
>0.9999
0.1092
0.0814
CX3CR1+ Int. Monocytes (%)
>0.9999
0.5425
>0.9999
CX3CR1+ NC Monocyte (%)
>0.9999
>0.9999
0.1353
CX3CR1+ T Cells (%)
0.4052
>0.9999
>0.9999
CD4+ TCM (%)
<0.0001
0.0114
0.1470
CD69 gMFI CD4 TEM
0.2321
0.0364
>0.9999
CD137 gMFI CD4 TEM
>0.9999
>0.9999
>0.9999
CD8+ TEMRA (%)
>0.9999
>0.9999
0.3152
CD8+ TEM (%)
>0.9999
0.5209
0.3164
CD69 gMFI CD8+ TEM
0.0130
0.0017
>0.9999
CD137 gMFI CD8+ TEM
>0.9999
0.9134
0.3703

783

**Supplementary Figure 4**. **Analysis of variance (Kruskall-Wallis) of remaining immune variables.** Analysis of variance of the values for immune variables (in percentages or gMFI) that were lesser influencers of the three first principal components and thus not included in the main figures.

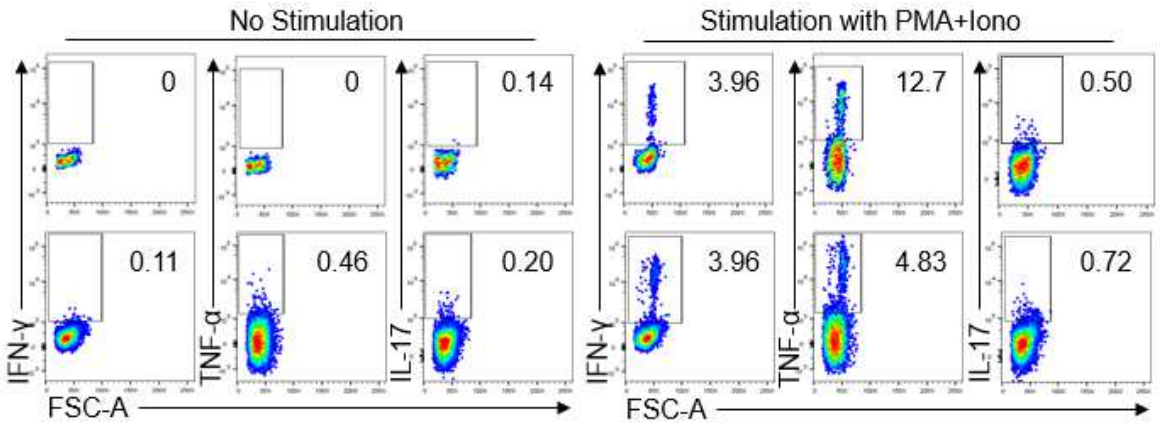


**Supplementary Figure 5**. **Control gate strategies for flow cytometry analysis of specific T cell responses.** Negative (DMSO) and positive (PMA+Ionomycin) controls gate strategies and representative plots of CD4+ or CD8+ T cell simulations.

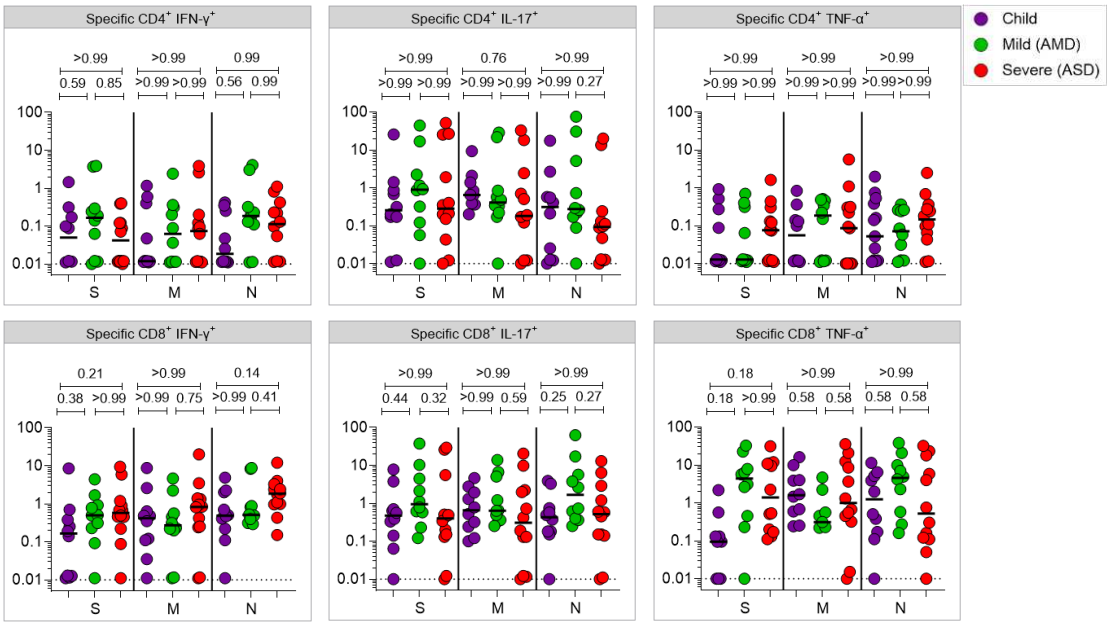


**Supplementary Figure 6. Comparison of specific T cell responses by effector T cell type among the groups.** Values of specific T cell responses (in percentages of positive CD4+ and CD8+ positive cytokine expressing cells in response to peptide pools) are plotted. Each dot represents a patient, color coded: children – purple, adult with mild disease – green, and adult with severe disease – red. All analyses are Kruskal-Wallis tests, and the p values are indicated in brackets.

**Supplementary Table 1.** Principal Component Analysis (PCA) variances and loading.

| **PCA all variables** | | | | | | | | | | | | | |
|---|---|---|---|---|---|---|---|---|---|---|---|---|---|
| Positive (loadings) | **PC1** | 1<br>Memory B IgG-IgM+ | 2<br>Naïve B cells | 3<br>cDC1 gMFI DR | **PC2** | 1<br>Treg | 2<br>mDC | 3<br>CD4+ TEMRA | **PC3** | 1<br>Naïve CD8+T | 2<br>Naïve CD4+T | 3<br>pDC | %cumul variance |
| | | 0.57 | 0.56 | 0.55 | | 0.53 | 0.45 | 0.40 | | 0.56 | 0.43 | 0.35 | |
| % variance explained | 12.16 | | | | 8.53 | | | | 8.12 | | | | 28.81 |
| Negative (loadings) | **PC1** | 1<br>B cells Ki67+ | 2<br>Plasma blasts | 3<br>DC gMFI CX3CR1 | **PC2** | 1<br>Eosino phils | 2<br>NK cells | 3<br>Granulo cytes | **PC3** | 1<br>DCs | 2<br>mDC gMFI DR | 3<br>cDC1 gMFI DR | |
| | | -0.71 | -0.58 | -0.60 | | -0.58 | -0.55 | -0.48 | | -0.64 | -0.60 | -0.60 | |
| **PCA Granu+Mono** | | | | | | | | | | | | | |
| Positive (loadings) | **PC1** | 1<br>Classical Monocytes | | 2<br>Intermediate Monocytes | | 3<br>Intermediate Monocytes CX3CR1+ | **PC2** | 1<br>Classical Monocytes CX3CR1+ | | | 2<br>CD16 Int Neutrophils | | %cumul variance |
| | | 0.84 | | 0.80 | | 0.75 | | 0.43 | | | 0.37 | | |
| % variance explained | 33.41 | | | | | | 16.96 | | | | | | 50.37 |
| Negative (loadings) | **PC1** | 1<br>- | | 2<br>- | | 2<br>- | **PC2** | 1<br>NC Monocytes | | | 2<br>NC Monocytes CX3CR1+ | | |
| | | - | | - | | - | | -0.66 | | | -0.64 | | |
| **PCA NK cells** | | | | | | | | | | | | | |
| Positive (loadings) | **PC1** | 1<br>NK Cells HLA-DR+ | | 2<br>NK Cells HLA-DR+ | | 3<br>NK CX3CR1+ | **PC2** | 1<br>NK T CX3CR1+ | | | 2<br>NK T | | %cumul variance |
| | | 0.85 | | 0.77 | | 0.73 | | 0.85 | | | 1.87 | | |
| % variance explained | 37.42 | | | | | | 29.94 | | | | | | 67.35 |
| Negative (loadings) | **PC1** | 1<br>- | | 2<br>- | | 3<br>- | **PC2** | 1<br>NK Cytotoxic | | | 2<br>NK Regulatory | | |
| | | - | | - | | - | | -0.43 | | | -0.34 | | |
| **PCA Dendritic Cells** | | | | | | | | | | | | | |
| Positive (loadings) | **PC1** | 1<br>mDCs gMFI CX3CR1 | | 2<br>cDC1 gMFI CX3CR1 | | 3<br>Non cDC1 gMFI CX3CR1 | **PC2** | 1<br>pDCs | | 2<br>mDCs | | 3<br>cDC1 | % cumul variance |
| | | 0.57 | | 0.51 | | 0.44 | | 0.59 | | 0.57 | | 0.23 | |

| | | | | | | | | | |
|---|---|---|---|---|---|---|---|---|---|
| % variance explained | 35.81 | | | | 27.36 | | | | 63.17 |
| Negative (loadings) | **PC1** | 1<br>mDCs gMFI DR | 2<br>DCs gMFI DR | 3<br>cDC1 gMFI DR | **PC2** | 1<br>cDC1 gMFI CX3CR1 | 2<br>Non cDC1 gMFI CX3CR1 | 3<br>cDC1 gMFI DR | |
| | | -0.85 | -0.85 | -0.83 | | -0.60 | -0.53 | -0.49 | |
| **PCA T cell activation + proliferation** | | | | | | | | | |
| Positive (loadings) | **PC1** | 1<br>CD4+ T HLADR+ GranB+Perf+ | 2<br>CD8+ T HLADR+ | 3<br>- | **PC2** | 1<br>CD4 T Ki67+ | | 2<br>CD8 T Ki67+ | % cumul variance |
| | | 0.76 | 0.64 | - | | 0.55 | | 0.43 | |
| % variance explained | 24.22 | | | | 19.97 | | | | 44.19 |
| Negative (loadings) | **PC1** | 1<br>CD8+ T Ki-67+ | 2<br>CD4+ T Ki67+ | 3<br>CD4+ T HLADR+ GranB+ Perf+ | **PC2** | 1<br>CD4+ T GranB+ Perf+ | | 2<br>CD8+ T GranB+ Perf+ | |
| | | -0.70 | -0.67 | -0.59 | | -0.64 | | -0.54 | |
| **PCA B cells** | | | | | | | | | |
| Positive (loadings) | **PC1** | 1<br>B IgG- IgM+ | 2<br>Naive B Cells | 3<br>Memory B IgG- IgM+ | **PC2** | 1<br>Memory B IgG+ IgM- | | 2<br>- | % cumul variance |
| | | 0.82 | 0.69 | 0.67 | | 0.75 | | - | |
| % variance explained | 31.2 | | | | 18.36 | | | | 49.56 |
| Negative (loadings) | **PC1** | 1<br>B IgG+ IgM- | 2<br>Plasmablasts | 3<br>B cells Ki-67+ | **PC2** | 1<br>B IgG+ IgM+ | | 2<br>Memory IgG+ IgM+ | |
| | | -0.75 | -0.67 | -0.59 | | -0.80 | | -0.57 | |
| **PCA T cell memory** | | | | | | | | | |
| Positive (loadings) | **PC1** | 1<br>CD4+ T Naive | | 2<br>CD8+ T Naive | **PC2** | 1<br>CD4+ TEMRA | | 2<br>CD8+ TEMRA | % cumul variance |
| | | 0.81 | | 0.79 | | 0.61 | | 0.41 | |
| % variance explained | 25.38 | | | | 17.1 | | | | 42.49 |
| Negative (loadings) | **PC1** | 1<br>CD4+ TEM | | 2<br>CD8+ TEM | **PC2** | 1<br>CD4+ TCM | | 2<br>CD8+ TEM | |
| | | -0.76 | | -0.61 | | -0.66 | | -0.50 | |

# Figures

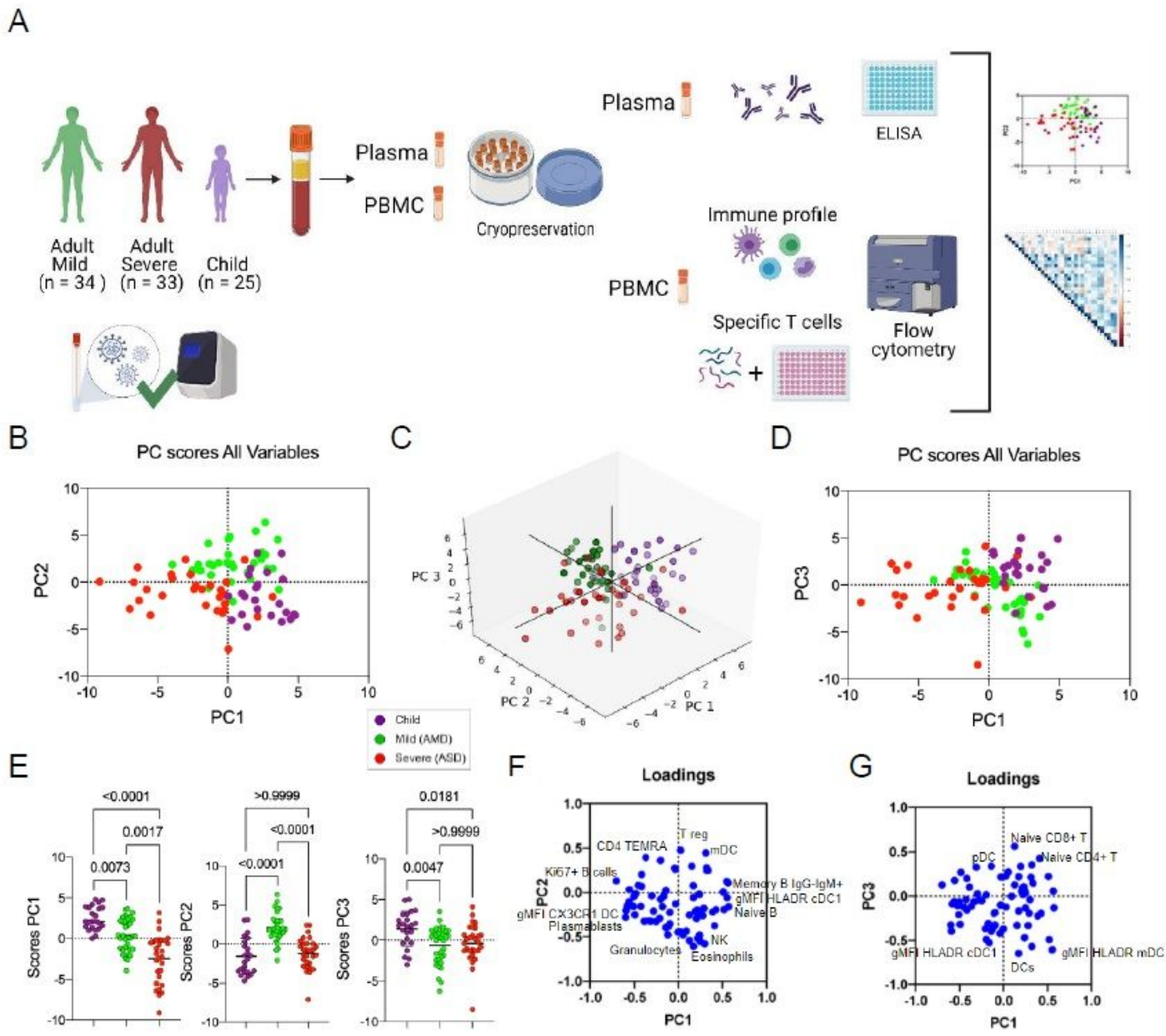


**Figure 1**

Experimental approach and differential immune profile of children, mild and adult patients by principal component analysis. A, Graphical representation of the study design; B-E, Principal component analysis of the clusters of pediatric (purple) and adult patients with mild (green) and severe (red) disease; each dot represents a patient, color coded. B, distribution of clusters by PC1 and PC2; C, 3D representation including PC1, 2 and 3; D, two-dimensional plot of patients according to PC3 by PC1; E, comparison of scores for each PC by analysis of variance (Kruskal-Wallis). F-G, Contribution of variables (loadings) to PC1xPC2 (F) and PC1xPC3 (G). Each blue dot is a variable. Variables with the highest contributions (negative or positive) to each PC are specified. P values are indicated over brackets.

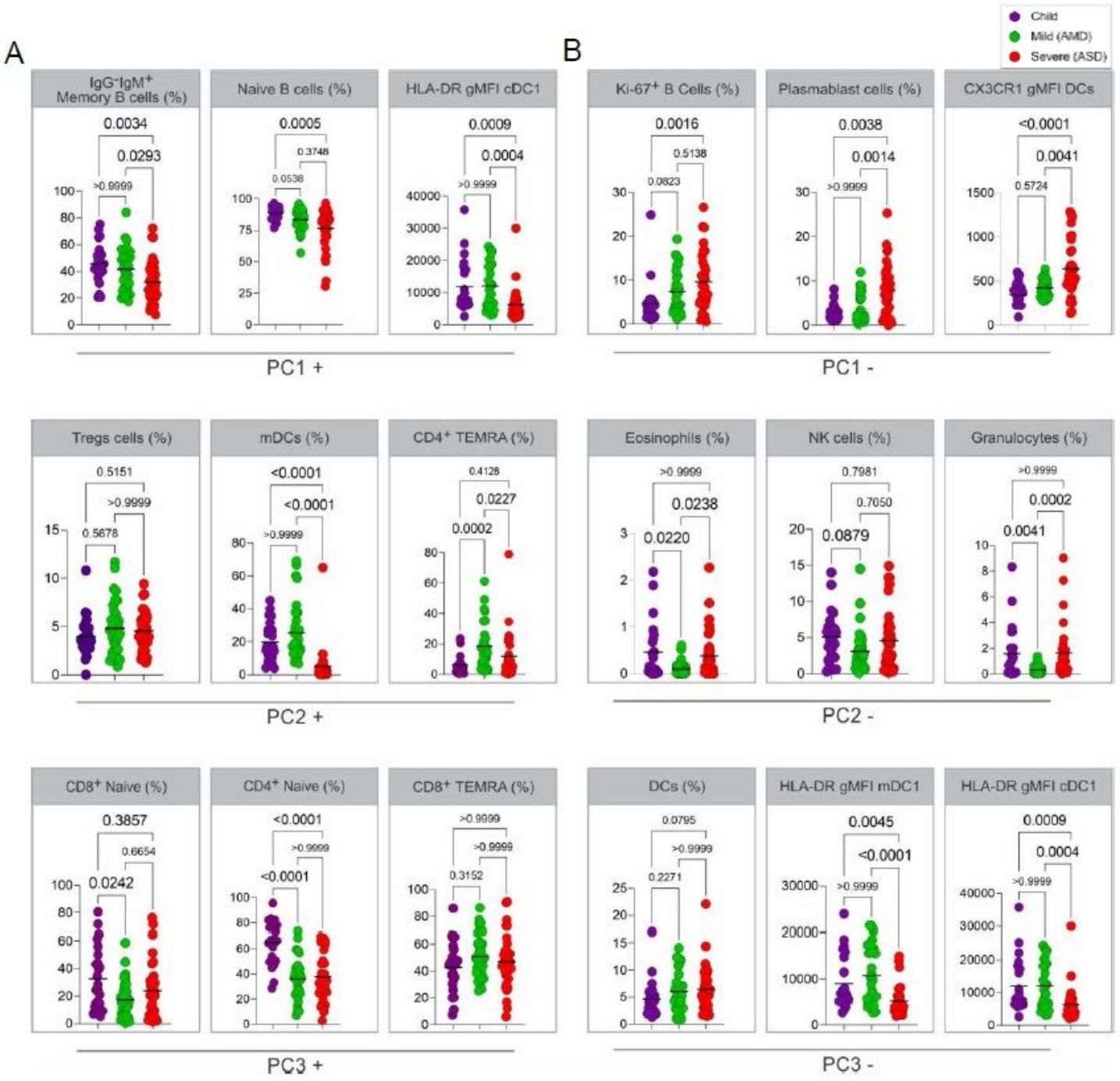


## Figure 2

Analysis of variance of the main variables contributing to principal components. A-B, Kruskal-Wallis tests comparing values of each of the three immune variables that presented the highest influences – either positive (A) or negative (B) for PC1, PC2 and PC3. Each dot represents a patient, color coded: children – purple, adult with mild disease – green, and adult with severe disease – red. P values are indicated over brackets.

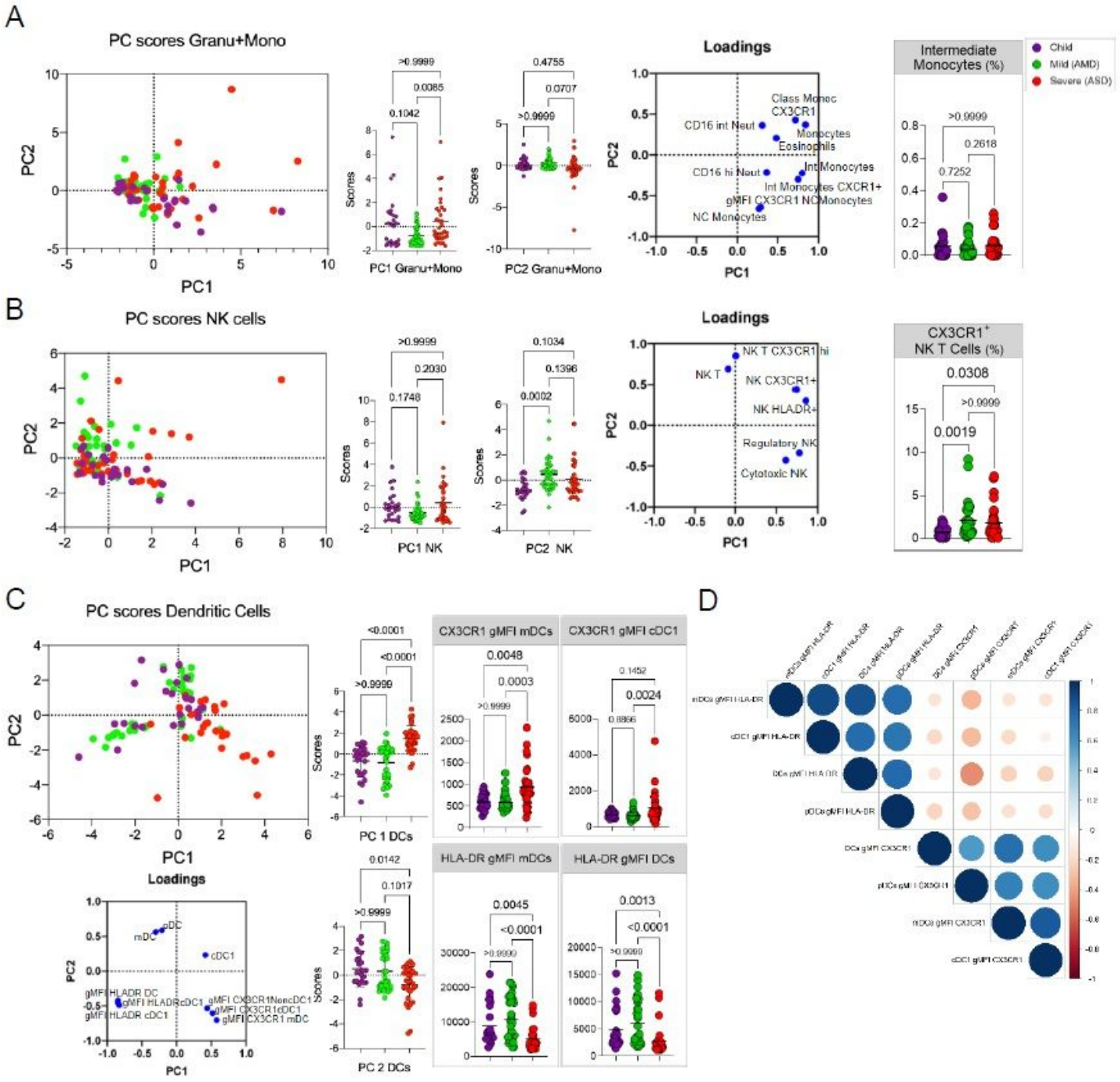


## Figure 3

Principal Component Analysis of innate cells immune signatures. A-G, Principal component analysis of the clusters of patients (each dot representing a patient, color coded), according to the immune signatures (A, Granu+Mono, Granulocytes and Monocytes; B, NK cells; C, Dendritic Cells; D, Spearman correlation analysis of HLA-DR and CX3CR1 expression in DCS. For each signature, are displayed the PCA plot of PC1xPC2, the differences in scores of individuals for each PC; the loadings of the main variables contributing to each PC and Kruskal-Wallis tests comparisons of the major contributing variables values for each group of patients.

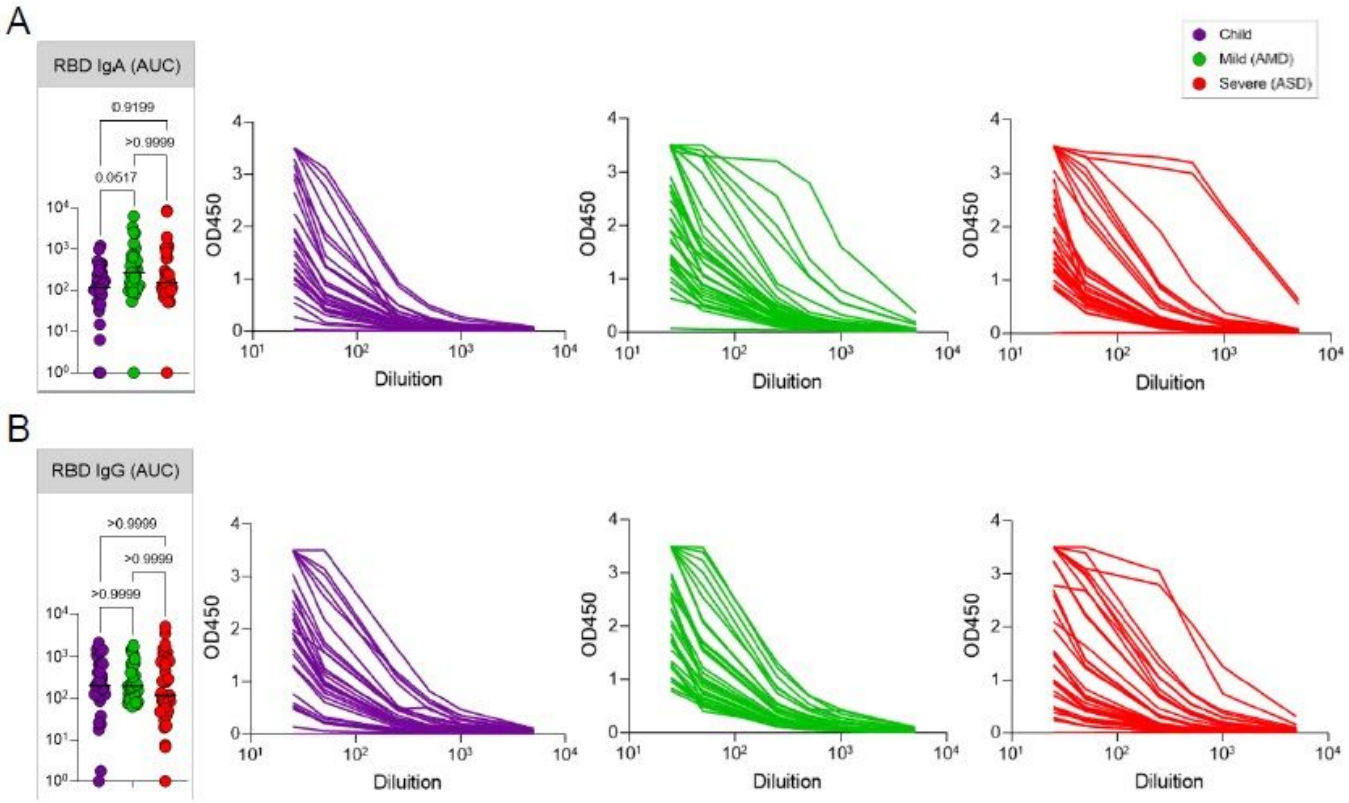


## Figure 4

Antibody responses. SARS-CoV-2 spike RBD IgA and IgG antibody titers determined by ELISA using serial dilutions of plasma. Individual titration curves for each individual (represented by a line, color coded) and analysis of variance (Kruskal-Wallis) of the values calculated as the area under the curve (AUC) for IgA (A) and IgG (B) are displayed. P values are displayed over brackets.

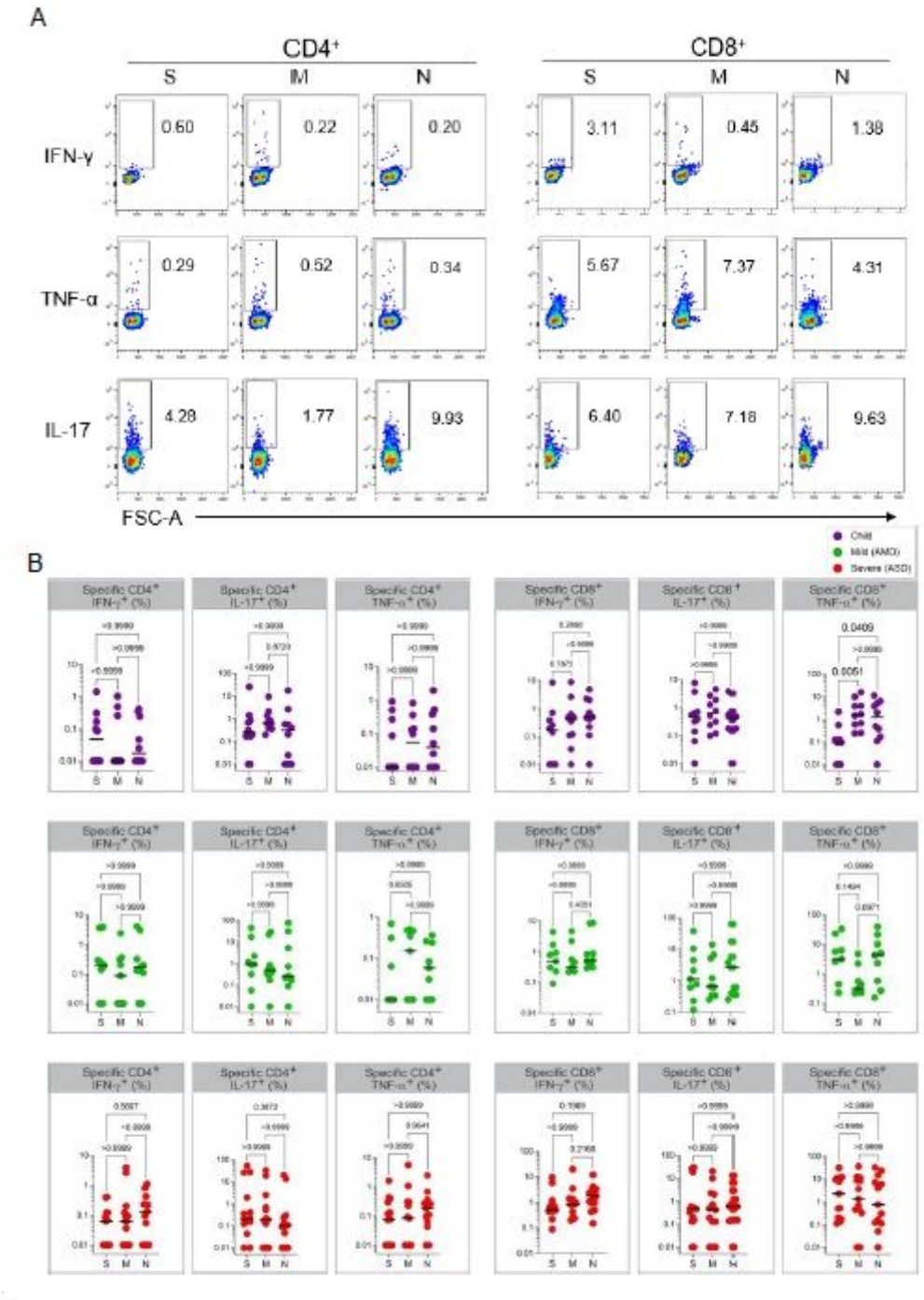


## Figure 5

Specific T cell responses. A, gating strategies and typical plots of CD4+ and CD8+ T cells stimulated with peptide pools from structural proteins spike (S), membrane (M) and nucleocapsid (N), and analyzed by flow cytometry for cytokine production. B, Comparisons of effector T cells in each group - percentages of CD4+ or CD8+ cells, producing INFy, TNFa or IL-17 in response to stimulation by each peptide pool. Each dot represents a patient, color coded: purple for children; green for adults with mild disease and red for

adults with severe disease. All analyses are Kruskal-Wallis tests, and the p values are indicated over brackets. Significant differences are indicated by p values in a higher font.

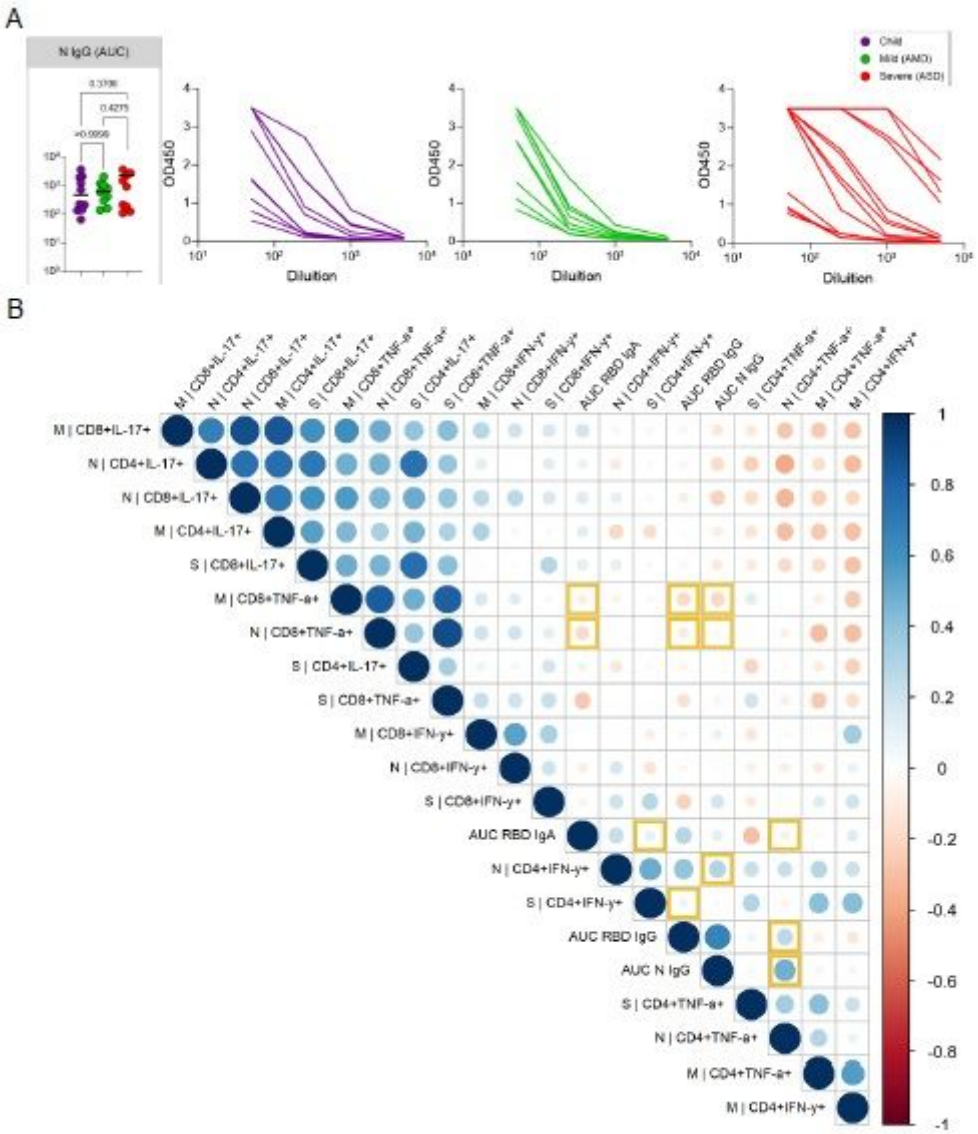


## Figure 6

Anti-N IgG response and correlation of specific responses. A, SARS-CoV-2 anti-N IgG antibody titers determined by ELISA using serial dilutions of plasma. Individual titration curves for each individual (represented by a line, color coded) and analysis of variance (Kruskal-Wallis) of the values calculated as the area under the curve (AUC) for IgG (A) are displayed. P values are displayed over brackets. B, Matrix representing a Spearman correlation analysis of specific effector T cells responses (in percentages of positive CD4+ and CD8+ positive cytokine expressing cells in response to peptide pools) and the antibody response to the RBD of the spike protein and to the N protein (represented as values for the AUC). Correlations between the specific effector CD8+ T and CD4+ T cells frequencies, and the antibody (AUC – area under the curve) values for the RBD and N protein are highlighted.